

MARTIN MARIETTA ENERGY SYSTEMS LIBRARIES



3 4456 0361435 5

CENTRAL RESEARCH LIBRARY
DOCUMENT COLLECTION

4

ORNL-2884
UC-34 - Physics and Mathematics
TID-4500 (15th ed.)

FOCUSING PROPERTIES OF INHOMOGENEOUS MAGNETIC
SECTOR FIELDS

M. M. Bretscher

CENTRAL RESEARCH LIBRARY
DOCUMENT COLLECTION
LIBRARY LOAN COPY
DO NOT TRANSFER TO ANOTHER PERSON
If you wish someone else to see this
document, send in name with document
and the library will arrange a loan.



OAK RIDGE NATIONAL LABORATORY
operated by
UNION CARBIDE CORPORATION
for the
U.S. ATOMIC ENERGY COMMISSION

Printed in USA. Price \$1.75. Available from the

Office of Technical Services
Department of Commerce
Washington 25, D. C.

LEGAL NOTICE

This report was prepared as an account of Government sponsored work. Neither the United States, nor the Commission, nor any person acting on behalf of the Commission:

- A. Makes any warranty or representation, expressed or implied, with respect to the accuracy, completeness, or usefulness of the information contained in this report, or that the use of any information, apparatus, method, or process disclosed in this report may not infringe privately owned rights; or
- B. Assumes any liabilities with respect to the use of, or for damages resulting from the use of any information, apparatus, method, or process disclosed in this report.

As used in the above, "person acting on behalf of the Commission" includes any employee or contractor of the Commission, or employee of such contractor, to the extent that such employee or contractor of the Commission, or employee of such contractor prepares, disseminates, or provides access to, any information pursuant to his employment or contract with the Commission, or his employment with such contractor.

ORNL-2884

Contract No. W-7405-eng-26

ANALYTICAL CHEMISTRY DIVISION

FOCUSING PROPERTIES OF INHOMOGENEOUS MAGNETIC SECTOR FIELDS

M. M. Bretscher

DATE ISSUED

MAR 29 1960

OAK RIDGE NATIONAL LABORATORY
Oak Ridge, Tennessee
operated by
UNION CARBIDE CORPORATION
for the
U. S. ATOMIC ENERGY COMMISSION

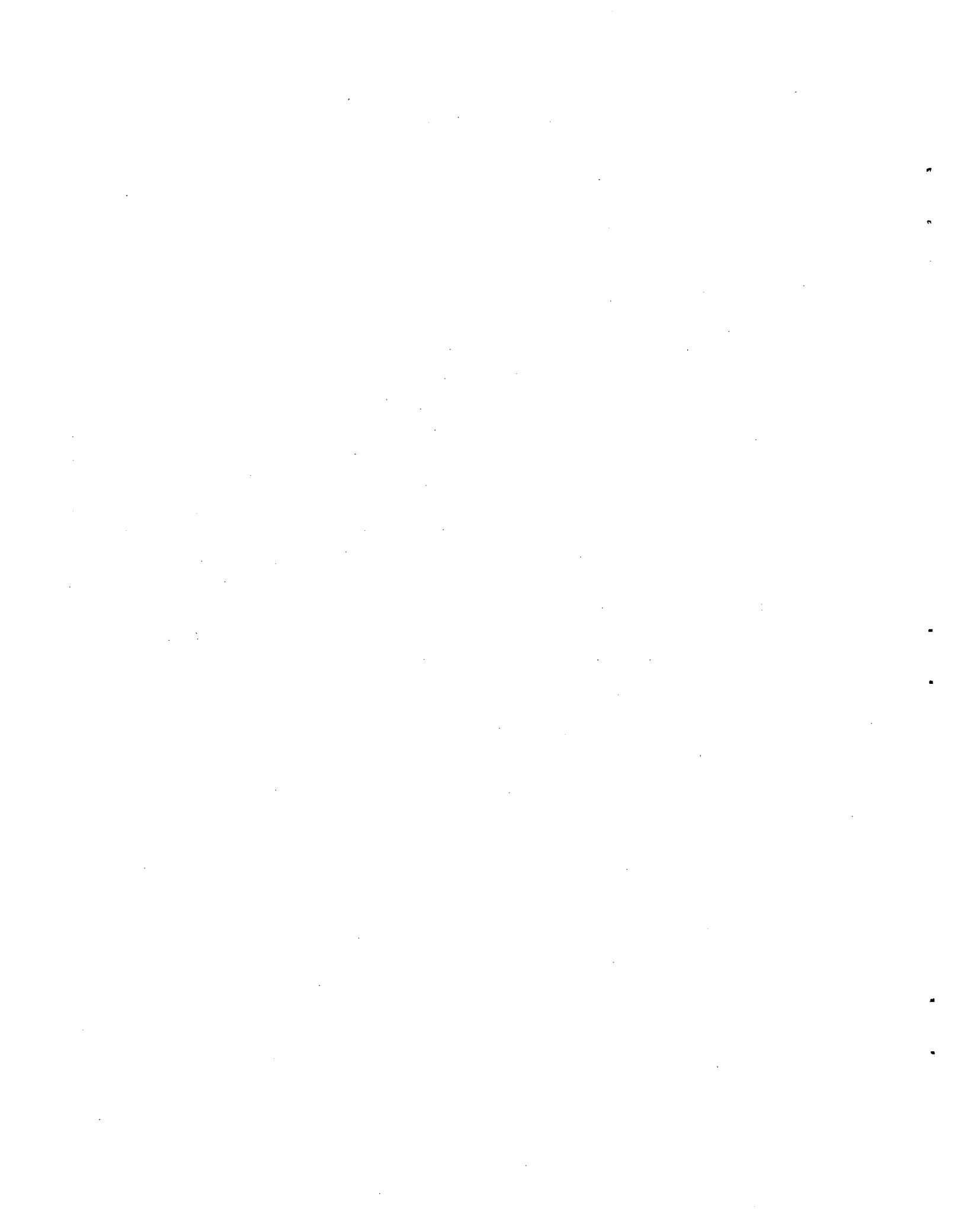


3 4456 0361435 5

100

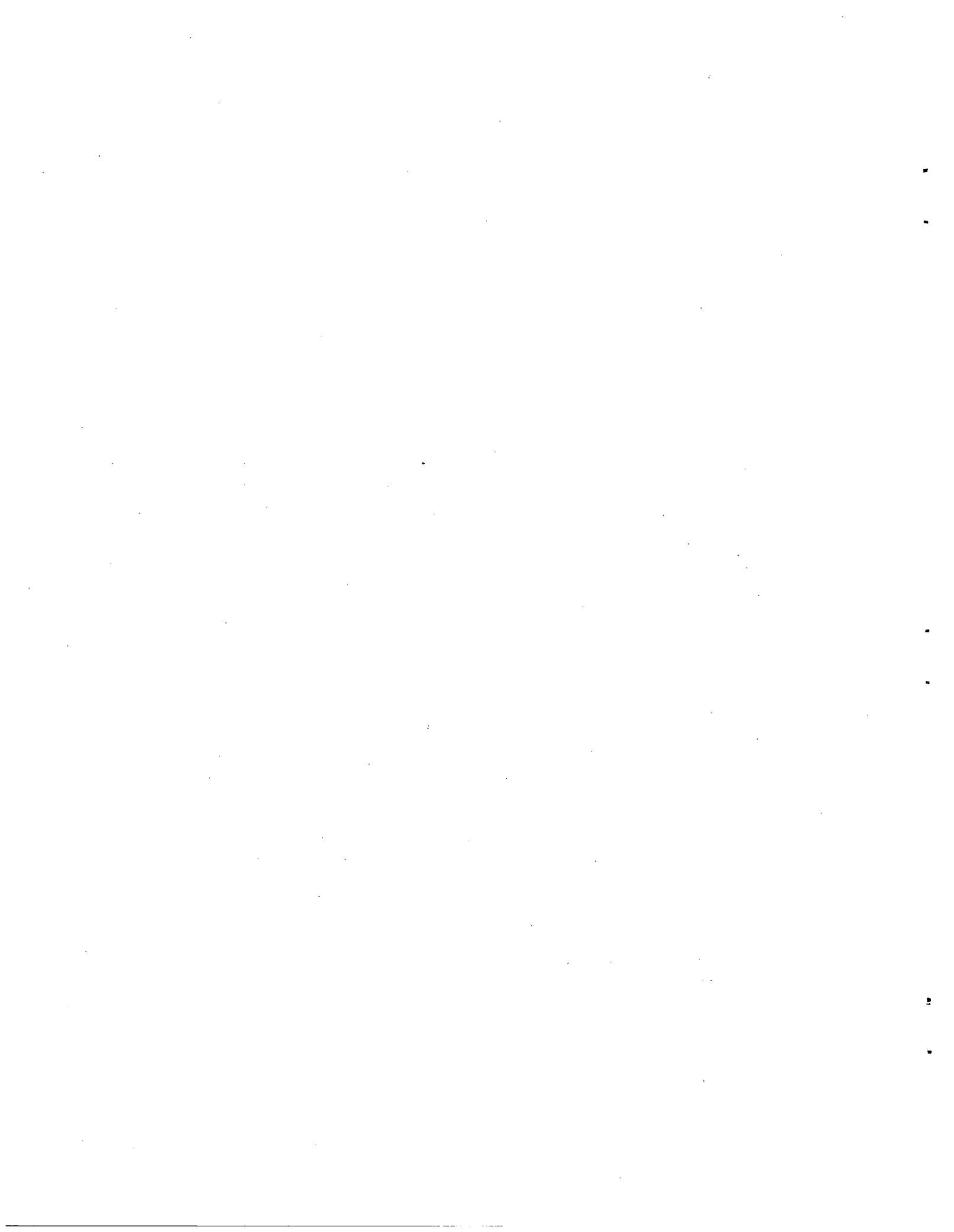
ABSTRACT

An investigation is made of the focusing properties of axially symmetric inhomogeneous magnetic sector fields with arbitrary circular boundaries. In first-order approximation the field is assumed to vary as r^{-n} ($0 \leq n < 1$). The equations of motion for the ion trajectories are developed from a least-action principle and solved through second-order approximation. Suitable expressions are derived for the horizontal and vertical focus positions, which are located outside the field boundaries. The mass dispersion and resolving power are found to vary as $(1 - n)^{-1}$ and so are considerably increased over the corresponding values for the homogeneous field ($n = 0$). Expressions for the second-order radial and vertical aberrations are derived. It is shown that the second-order radial aberration may be eliminated by proper shaping of the magnetic field and/or field boundaries. An equation is developed for the profile of the pole faces required to produce the desired field. The results are finally modified to account for the defocusing action of the magnetic fringing field. A numerical example is presented for a symmetrical spectrometer having a 90° sector field with $n = \frac{1}{2}$. For this case simultaneous double directional and second-order radial focusing are possible.



CONTENTS

1. INTRODUCTION	1
2. THE MAGNETIC FIELD	2
3. THE EULER-LAGRANGE EQUATIONS OF MOTION	6
4. ION TRAJECTORIES WITHIN THE SECTOR FIELD	7
Zero-Order Approximation	8
First-Order Approximation	8
Second-Order Approximation	8
Solution to Radial Equation	9
Solution to Axial Equation	12
5. ION TRAJECTORIES IN FIELD-FREE IMAGE SPACE	13
6. IMAGE PROPERTIES.....	18
Focal Distances	18
Magnification	19
Mass Dispersion	20
Chromatic Aberration	21
Solid Angle.....	21
Second-Order Radial Aberration	22
Resolution	24
Vertical Aberration	25
7. IMAGE PROPERTIES FOR AN INFLECTION SPECTROMETER.....	25
Radial Focusing, Magnification and Mass Dispersion.....	25
Vertical Focusing	28
8. THE SYMMETRIC ARRANGEMENT.....	29
9. SIMULTANEOUS DOUBLE DIRECTIONAL AND SECOND-ORDER RADIAL FOCUSING.....	31
10. FRINGE FIELD EFFECTS	32
11. A NUMERICAL ILLUSTRATION	40
12. CONCLUSION	44
APPENDIX A. SUMMARY OF NOTATION.....	46
APPENDIX B. IMAGE DISPLACEMENT DUE TO FRINGING FIELD – A SIMPLIFIED ANALYSIS	48
APPENDIX C. THE HOMOGENEOUS FIELD SPECTROMETER.....	49



FOCUSING PROPERTIES OF INHOMOGENEOUS MAGNETIC SECTOR FIELDS

M. M. Bretscher¹

1. INTRODUCTION

Axially symmetric nonuniform magnetic analyzers in which the field varies as $r^{-1/2}$ have been used to achieve double directional focusing and improved resolution in beta-ray spectrometers²⁻⁷ and in nuclear spectrometers.⁸⁻¹⁴ Theoretical calculations of the ion-optical properties of these magnetic lens systems in which both the source and collector are located within the field boundaries have been treated by several authors.¹⁵⁻²¹

First-order focus conditions for inhomogeneous magnetic sector fields, wherein the source and image lie entirely outside the field region, have been calculated by Svartholm,²² Judd,²³ Rosenblum,²⁴ and Sternheimer.²⁵ Alekseevski *et al.*²⁶ recognized that a magnetic field varying in the midplane as r^{-n} ($0 \leq n < 1$) could be used to increase the resolving power and mass dispersion by a factor of $(1 - n)^{-1}$. Several mass spectrometers using this principle have been reported in the Russian literature.²⁷ Svartholm²⁸ and Fischer²⁹ have proposed mass spectrometers employing crossed nonuniform electric and magnetic fields as a means of obtaining simultaneous velocity and two-directional focusing of charged particles.

¹Summer Research Participant from Valparaiso University, Valparaiso, Ind.

²K. Siegbahn and N. Svartholm, *Nature* 157, 872 (1946).

³F. M. Beiduk and E. J. Konopinski, *Rev. Sci. Instr.* 19, 594 (1948).

⁴F. N. D. Kurie, J. S. Osoba, and L. Slack, *Rev. Sci. Instr.* 19, 771 (1948).

⁵A. Hedgran, K. Siegbahn, and N. Svartholm, *Proc. Phys. Soc. (London)* A63, 960 (1950).

⁶N. F. Verster, *Physica* 16, 815 (1950).

⁷E. Arbman and N. Svartholm, *Arkiv Fysik* 10, 1 (1956).

⁸C. W. Snyder *et al.*, *Phys. Rev.* 74, 1564 (1948).

⁹C. W. Snyder *et al.*, *Rev. Sci. Instr.* 21, 852 (1950).

¹⁰C. Mileikowsky, *Arkiv Fysik* 4, 337 (1952); 7, 33, 57 (1954).

¹¹S. Rubin and D. C. Sachs, *Rev. Sci. Instr.* 26, 1029 (1955).

¹²R. Pauli, *Arkiv Fysik* 10, 175 (1956).

¹³E. E. Chambers and R. Hofstadter, *Phys. Rev.* 103, 1454 (1956).

¹⁴L. Bianchi, E. Cotton, and C. Mileikowsky, *Nuclear Instr.* 3, 69 (1958).

¹⁵N. Svartholm and K. Siegbahn, *Arkiv Mat. Astron. Fysik* 33A, No. 21 (1946).

¹⁶N. Svartholm, *Arkiv Mat. Astron. Fysik* 33A, No. 24 (1946).

¹⁷F. B. Shull and D. M. Dennison, *Phys. Rev.* 71, 681 (1947); 72, 256 (1947).

¹⁸H. W. Franke, *Österr. Ing.-Arch.* 5, 371 (1951); 6, 105 (1952).

¹⁹H. Grümm, *Acta Phys. Austriaca* 8, 119 (1953).

²⁰P. H. Stoker *et al.*, *Physica* 20, 337 (1954).

²¹G. E. Lee-Whiting and E. A. Taylor, *Can. J. Phys.* 35, 1 (1957).

²²N. Svartholm, *Arkiv Fysik* 2, 115 (1950).

²³D. L. Judd, *Rev. Sci. Instr.* 21, 213 (1950).

²⁴E. S. Rosenblum, *Rev. Sci. Instr.* 21, 586 (1950).

²⁵R. M. Sternheimer, *Rev. Sci. Instr.* 23, 629 (1952).

²⁶N. E. Alekseevsky *et al.*, *Doklady Akad. Nauk S.S.S.R.* 100, 229 (1955).

²⁷A. V. Dubrovina and G. V. Balabina, *Doklady Akad. Nauk S.S.S.R.* 102, 719 (1955).

²⁸N. Svartholm, *Arkiv Fysik* 2, 195 (1950).

²⁹D. Fischer, *Z. Physik* 133, 471 (1952).

Recently, Ikegami³⁰ and Tasman and Boerboom³¹ have examined second-order aberrations arising in the focusing of charged particles by inhomogeneous magnetic sector fields. The effect on the second-order aberration terms due to the fringing field has been estimated by Judd and Bludman³² for the case of a 180° double-focusing alpha-particle spectrometer.

A mass spectrometer using an inhomogeneous magnetic field with index $n = 0.80$ has recently been built at this Laboratory, while a second instrument, taking advantage of the double directional focusing property characteristic of $n = \frac{1}{2}$ fields, is currently under construction. It seemed desirable, therefore, to carefully re-examine the ion-optical properties characteristic of nonuniform magnetic fields. In this report, the equations of motion for the ion trajectories are developed from a least-action principle analogous to the Fermat principle in geometric optics. These equations are solved through second-order approximation. Suitable expressions for the mass dispersion, the resolving power, and the horizontal and vertical focusing positions are derived. It is shown that second-order aberration terms may be eliminated by proper shaping of the magnetic field, and an equation is developed for the profile of the pole faces required to produce this desired field. Finally, it is shown how the results must be modified to account for the defocusing action of the fringing field.

2. THE MAGNETIC FIELD

We shall express the equations of motion for the ion trajectories within the magnetic induction field \mathbf{B} in terms of the cylindrical coordinate system r, ϕ, z . On the midplane ($z = 0$) the field is directed along the z axis so that a positively charged particle will move in the direction of increasing ϕ .

The magnetic field is assumed to have cylindrical symmetry with respect to the z axis and mirror symmetry with respect to the median plane $z = 0$. On this plane the field may be expressed by a series expansion in the vicinity of the circular equilibrium orbit of radius r_0 . Thus

$$B_\sigma(\rho, 0) = B_0(1 - n\rho + b\rho^2 - c\rho^3 + d\rho^4 - \dots) ,$$

where we define the dimensionless coordinates ρ and σ as

$$\rho \equiv \frac{r - r_0}{r_0} , \quad \sigma \equiv \frac{z}{r_0} , \quad (1)$$

and B_0 is the induction field at $\rho = \sigma = 0$. If the field in the median plane is assumed to vary as r^{-n} , the identification $b = n(n+1)/2$ can be made. However, we shall assume that $B_0, b, c,$ and d are experimentally adjustable parameters.

³⁰H. Ikegami, *Rev. Sci. Instr.* **29**, 943 (1958).

³¹H. A. Tasman and A. J. H. Boerboom, *Z. Naturforsch.* **14a**, 121 (1959).

³²D. L. Judd and S. A. Bludman, *Nuclear Instr.* **1**, 46 (1957).

Within the gap $\nabla \times \mathbf{B} = 0$ and $\nabla \cdot \mathbf{B} = 0$, from which it follows that

$$B_\rho(\rho, \sigma) = B_0 \left[-n\sigma + 2b\rho\sigma - 3c\rho^2\sigma + 4d\rho^3\sigma - \frac{1}{6}(n+2b-6c)\sigma^3 + \frac{1}{3}(n+2b+3c-12d)\rho\sigma^3 - \dots \right] \quad (2)$$

and

$$B_\sigma(\rho, \sigma) = B_0 \left[1 - n\rho + b\rho^2 - c\rho^3 + d\rho^4 - \dots + \frac{1}{2}(n-2b)\sigma^2 - \frac{1}{2}(n+2b-6c)\rho\sigma^2 + \frac{1}{2}(n+2b+3c-12d)\rho^2\sigma^2 - \frac{1}{24}(n+2b+12c-24d)\sigma^4 + \dots \right] \quad (3)$$

We next evaluate, to third-order approximation, the magnetic vector potential \mathbf{A} which will generate this field. Since the magnetic field $\mathbf{B} = \nabla \times \mathbf{A}$ is independent of ϕ ,

$$B_\phi = \frac{\partial A_r}{\partial z} - \frac{\partial A_z}{\partial r} = 0 \quad ,$$

and we may choose the vector potential so that the components A_r and A_z vanish. It is apparent from (2) and (3) that the nonvanishing component of the vector potential may be expanded in a power series of the form

$$A_\phi = \sum_{i,j=0}^{\infty} A_{ij} \rho^i \sigma^j \quad . \quad (4)$$

Now the coefficient A_{00} corresponds to the vector potential of a homogeneous field with $B_\sigma = B_0$. Hence

$$A_{00} = \frac{B_0}{r_0} \int_0^{r_0} r \, dr = \frac{1}{2} B_0 r_0 \quad .$$

From the defining equation $\mathbf{B} = \nabla \times \mathbf{A}$,

$$B_\rho = -\frac{1}{r_0} \frac{\partial A_\phi}{\partial \sigma} = -\frac{1}{r_0} \sum_{i,j} j A_{ij} \rho^i \sigma^{j-1} \quad (5)$$

and

$$B_\sigma = \frac{1}{r_0(1+\rho)} \frac{\partial}{\partial \rho} (1+\rho) A_\phi = \frac{1}{r_0} \left(\sum_{i,j} i A_{ij} \rho^{i-1} \sigma^j + \frac{1}{1+\rho} \sum_{i,j} A_{ij} \rho^i \sigma^j \right) \quad . \quad (6)$$

The remaining coefficients A_{ij} are evaluated by comparing Eqs. (2) and (3) with (5) and (6).

The results are:

$$\left. \begin{aligned}
 A_{01} &= A_{11} = A_{21} = A_{31} = A_{03} = A_{13} = 0 , \\
 A_{00} &= \frac{1}{2} B_0 r_0 , & A_{30} &= \frac{1}{6} B_0 r_0 (n + 2b) , \\
 A_{10} &= \frac{1}{2} B_0 r_0 , & A_{12} &= - b B_0 r_0 , \\
 A_{02} &= \frac{1}{2} n B_0 r_0 , & A_{22} &= \frac{3}{2} c B_0 r_0 , \\
 A_{20} &= - \frac{1}{2} n B_0 r_0 , & A_{40} &= - \frac{1}{12} B_0 r_0 (2n + b - 3c) .
 \end{aligned} \right\} \quad (7)$$

Since $\nabla \times \mathbf{B} = 0$ within the pole gap, a magnetic scalar potential function ϕ_m exists such that

$$\mathbf{B} = - \nabla \phi_m . \quad (8)$$

We may express ϕ_m in terms of a power series in ρ and σ . Since \mathbf{B} has mirror symmetry with respect to the $z = 0$ plane, only odd powers of σ appear in the expansion of ϕ_m . Thus

$$\phi_m = \sum_{i,j=0}^{\infty} a_{ij} \rho^i \sigma^{2j+1} , \quad (9)$$

and from (8),

$$\begin{aligned}
 B_\rho &= - \frac{1}{r_0} \frac{\partial \phi_m}{\partial \rho} = - \frac{1}{r_0} \sum_{i,j} i a_{ij} \rho^{i-1} \sigma^{2j+1} , \\
 B_\sigma &= - \frac{1}{r_0} \frac{\partial \phi_m}{\partial \sigma} = - \frac{1}{r_0} \sum_{i,j} a_{ij} (2j+1) \rho^i \sigma^{2j} ,
 \end{aligned} \quad (10)$$

which permits one to evaluate the a_{ij} coefficients. Including terms through fifth order, the scalar potential becomes

$$\begin{aligned}
 \phi_m = B_0 r_0 \left[- \sigma + n \rho \sigma - b \rho^2 \sigma - \frac{1}{6} (n - 2b) \sigma^3 + c \rho^3 \sigma + \frac{1}{6} (n + 2b - 6c) \rho \sigma^3 - \right. \\
 \left. - d \rho^4 \sigma - \frac{1}{6} (n + 2b + 3c - 12d) \rho^2 \sigma^3 + \frac{1}{120} (n + 2b + 12c - 24d) \sigma^5 + \dots \right] . \quad (11)
 \end{aligned}$$

Equation (11) is used to calculate the magnetic equipotential surfaces. If the pole shoe is made of a material of large permeability at the field strength used, the pole surface is one of constant magnetic scalar potential. For this surface we put

$$\phi_m(\rho, \sigma) = \text{const} = - B_0 r_0 \xi , \quad (12)$$

where the constant ξ is given by (11) with $\rho = 0$ and $\sigma = g_0/(2r_0)$; g_0 is the gap width at the

equilibrium radius r_0 . Thus

$$\xi = \frac{1}{2} \frac{g_0}{r_0} + \frac{1}{48} (n - 2b) \left(\frac{g_0}{r_0} \right)^3 + \dots \quad (13)$$

Computing σ as a function of ρ from (11) by successive approximations we obtain

$$\sigma = \xi \left[1 - \frac{1}{6} (n - 2b) \xi^2 \right] + \left[n + \frac{1}{6} (-4n^2 + 4nb + n + 2b - 6c) \xi^2 \right] \xi \rho + (n^2 - b) \xi \rho^2 + (n^3 - 2nb + c) \xi \rho^3 + \dots \quad (14)$$

Since ξ and ρ are considerably less than unity in most cases of practical interest, (14) rapidly converges and gives the equation for the profile of the pole shoes required to produce the desired field shape (2) and (3). As will be shown later, the parameter b is so chosen as to minimize the second-order radial aberration terms. On the other hand, c and d are arbitrary and may be set equal to zero.

Pole pieces with conical surfaces may be used to satisfy first-order focusing requirements. The profile of the pole face is then a straight line, and hence the slope $d\sigma/d\rho$, evaluated from (14), must be constant. Thus the coefficients of the ρ^2 and ρ^3 terms must vanish, and we have

$$\frac{d\sigma}{d\rho} = \text{const} = n\xi + \frac{1}{6} n\xi^3 (1 - 2n - 2n^2) \quad (15)$$

As is seen from (13), $\xi \approx \frac{1}{2} g_0 / r_0 \ll 1$, and so

$$n \approx \frac{2r_0}{g_0} \tan \frac{\gamma}{2} \quad (16)$$

where γ is the angle between the extensions of the conical pole pieces, as illustrated in Fig. 1.

UNCLASSIFIED
ORNL-LR-DWG 45140

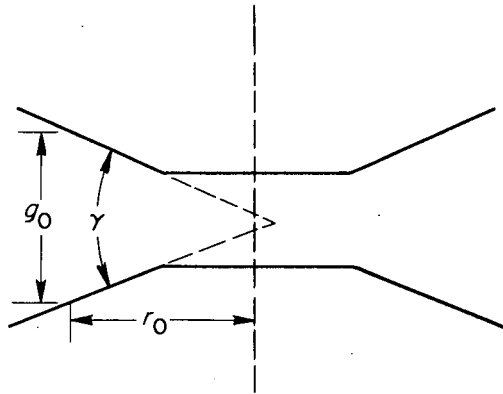


Fig. 1. Pole Shoes with Conical Faces.

3. THE EULER-LAGRANGE EQUATIONS OF MOTION

In nonrelativistic mechanics the principle of least action,³³ for conservative forces, may be written as

$$\Delta \int 2T dt = \Delta \int \mathbf{p} \cdot d\mathbf{s} = 0 ,$$

where T is the kinetic energy of the particle, \mathbf{p} the momentum, and $d\mathbf{s}$ an element of displacement along the path. For the velocity-dependent magnetic force, one must replace the momentum in the above equation by $\mathbf{p} - q\mathbf{A}$, where q is the charge of the ion and \mathbf{A} the magnetic vector potential. Thus

$$\Delta \int (\mathbf{p} - q\mathbf{A}) \cdot d\mathbf{s} = 0 . \quad (17)$$

This is the Schwarzschild³⁴ variation principle and applies to the motion of charged particles in a magnetic field. It is analogous to the Fermat principle in geometric optics.

Since the magnetic force always acts at right angles to the ion velocity \mathbf{v} , the component of momentum along the path is constant. Equation (17) then becomes

$$\Delta \int \left(ds - \frac{q\mathbf{v} \cdot \mathbf{A}}{p} dt \right) = \Delta \int \left(ds - \frac{qrA_\phi}{p} d\phi \right) = \Delta \int \left(ds - \frac{qrA_\phi}{\sqrt{2mqV}} d\phi \right) = 0 ,$$

where m is the mass of the ion and V the potential difference through which it has been accelerated. With

$$ds = [(dr)^2 + r^2(d\phi)^2 + (dz)^2]^{1/2} = (r'^2 + r^2 + z'^2)^{1/2} d\phi ,$$

where the primes represent differentiation with respect to ϕ , the Schwarzschild variational principle becomes

$$\Delta \int \left(\sqrt{r'^2 + r^2 + z'^2} - \sqrt{\frac{q}{2mV}} rA_\phi \right) d\phi = 0 ,$$

or, in terms of the dimensionless coordinates ρ and σ ,

$$\Delta \int \left(\sqrt{\rho'^2 + (1+\rho)^2 + \sigma'^2} - \sqrt{\frac{q}{2mV}} (1+\rho) A_\phi \right) d\phi = 0 . \quad (18)$$

The Euler-Lagrange equations for the orbit are therefore

$$\begin{aligned} \frac{d}{d\phi} \left(\frac{\partial F}{\partial \rho'} \right) - \frac{\partial F}{\partial \rho} &= 0 , \\ \frac{d}{d\phi} \left(\frac{\partial F}{\partial \sigma'} \right) - \frac{\partial F}{\partial \sigma} &= 0 , \end{aligned} \quad (19)$$

³³See, for example, H. Goldstein, *Classical Mechanics*, chap. 7, Addison-Wesley, Cambridge, Mass., 1950.

³⁴K. Schwarzschild, *Nachr. kgl. Ges. Wiss. Göttingen, Math.-physik. Kl.* 1903, 126.

where F is the integrand of Eq. (18). Defining

$$\eta \equiv \sqrt{\frac{q}{2mV}} , \quad (20)$$

we now expand F through third order (in ρ and σ), making use of (4) for the vector potential. Thus ...

$$\begin{aligned} F &= \sqrt{(1+\rho)^2 + (\rho'^2 + \sigma'^2)} - \eta(1+\rho) A_\phi \\ &= 1 + \rho + \frac{1}{2}(\rho'^2 + \sigma'^2) - \frac{1}{2}\rho(\rho'^2 + \sigma'^2) + \dots - \eta(1+\rho) \sum_{i,j} A_{ij} \rho^i \sigma^j \\ &= \frac{1}{2}(\rho'^2 + \sigma'^2)(1-\rho) + F_{00} + F_{10}\rho + F_{20}\rho^2 + F_{02}\sigma^2 + F_{30}\rho^3 + F_{12}\rho\sigma^2 + \dots , \quad (21) \end{aligned}$$

where, with the aid of (7),

$$\begin{aligned} F_{00} &= 1 - \eta A_{00} = 1 - \frac{1}{2} \eta B_0 r_0 , \\ F_{10} &= 1 - \eta(A_{00} + A_{10}) = 1 - \eta B_0 r_0 , \\ F_{20} &= -\eta(A_{20} + A_{10}) = -\frac{\eta B_0 r_0}{2} (1-n) , \\ F_{02} &= -\eta A_{02} = -\frac{1}{2} n \eta B_0 r_0 , \\ F_{30} &= -\eta(A_{30} + A_{20}) = \frac{1}{3} \eta B_0 r_0 (n-b) , \\ F_{12} &= -\eta(A_{12} + A_{02}) = -\eta B_0 r_0 \left(\frac{n}{2} - b \right) . \end{aligned} \quad (22)$$

These results are in agreement with those given by Glaser.³⁵

4. ION TRAJECTORIES WITHIN THE SECTOR FIELD

Successive approximations for the ion trajectories are found by substituting F into the Euler-Lagrange equations and retaining terms in F up to one order higher than that of the approximation wanted. One defines the order of approximation by the highest degree in ρ_0 , σ_0 , ρ'_0 , and σ'_0 (the values of ρ , σ , ρ' , and σ' at $\phi = 0$) appearing in the expression for the ion paths.

³⁵W. Glaser, *Handbuch der Physik* (ed. by S. Flügge), vol 33, p 308 ff., Springer-Verlag, Berlin, 1956.

Zero-Order Approximation

Keeping terms through first order in F , we obtain from Eqs. (19), (21), and (22) $F_{10} = 0$, and so

$$r_0 = \frac{1}{\eta_0 B_0} . \quad (23)$$

This gives the radius of the central path for ions of mass m_0 , velocity v_0 , and charge q_0 .

First-Order Approximation

Retaining terms through second order in F , the Euler-Lagrange equations become

$$\begin{aligned} \rho'' - 2\rho F_{20} &= F_{10} , \\ \sigma'' - 2\sigma F_{02} &= 0 , \end{aligned}$$

where $\rho'' \equiv d^2\rho/d\phi^2$ and $\sigma'' \equiv d^2\sigma/d\phi^2$. The solutions to these equations are

$$\begin{aligned} \rho &= C_1 \sin k_1 \phi + C_2 \cos k_1 \phi - \frac{1}{2} \frac{F_{10}}{F_{20}} , \\ \sigma &= K_1 \sin k_2 \phi + K_2 \cos k_2 \phi , \end{aligned} \quad (24)$$

where $k_1^2 \equiv -2F_{20}$ and $k_2^2 \equiv -2F_{02}$. The constants C_1 , C_2 , K_1 , and K_2 are determined from the initial conditions. Thus

$$\begin{aligned} \rho &= (1-n)^{-1/2} \rho'_0 \sin k_1 \phi + \left(\rho_0 + \frac{1}{2} \frac{F_{10}}{F_{20}} \right) \cos k_1 \phi , \\ \sigma &= n^{-1/2} \sigma'_0 \sin k_2 \phi + \sigma_0 \cos k_2 \phi . \end{aligned} \quad (25)$$

In the radial plane the orbit (through first-order approximation) is seen to oscillate about the central path of radius r_0 with a frequency $(1-n)^{1/2} d\phi/dt$, while a second oscillation occurs about the median plane, $z = 0$, with a frequency $n^{1/2} d\phi/dt$. These observations are in agreement with those of Kerst.³⁶

Second-Order Approximation

Now keeping terms through third order in F , the Euler-Lagrange orbit equations reduce to

$$\rho'' + k_1^2 \rho = \rho \rho'' + \frac{1}{2} (\rho'^2 - \sigma'^2) + F_{10} + 3F_{30} \rho^2 + F_{12} \sigma^2 , \quad (26)$$

$$\sigma'' + k_2^2 \sigma = \rho \sigma'' + \sigma' \rho' + 2F_{12} \sigma \rho . \quad (27)$$

³⁶D. W. Kerst and R. Serber, *Phys. Rev.* **60**, 53 (1941).

Note that all the terms in ρ and σ on the right-hand side of these equations are of second degree, whereas those on the left-hand side are all of first degree. We may therefore approximate the right-hand terms making use of the first-order solutions given by (25). Thus (26) and (27) may be written as

$$\rho'' + k_1^2 \rho = f_1(\phi) , \quad (28)$$

$$\sigma'' + k_2^2 \sigma = f_2(\phi) , \quad (29)$$

where f_1 and f_2 are known functions of ϕ . Equations (28) and (29) may be solved by the method of variation of parameters. Thus

$$\rho = A_1(\phi) \sin k_1 \phi + B_1(\phi) \cos k_1 \phi , \quad (30)$$

where

$$A_1 = \frac{1}{k_1} \left[\int f_1(\phi) \cos k_1 \phi d\phi + C_3 \right] , \quad (31)$$

$$B_1 = -\frac{1}{k_1} \left[\int f_1(\phi) \sin k_1 \phi d\phi + C_4 \right] .$$

An analogous solution may be written for σ .

Solution to Radial Equation. – Lengthy though straightforward integration of (31) gives the second-order approximation for ρ , which may be written in the form

$$\begin{aligned} \rho(\phi) = H_0 + \rho_0 H_1 + \rho_0' H_2 + \rho_0^2 H_{11} + \rho_0 \rho_0' H_{12} + \rho_0'^2 H_{22} + \sigma_0^2 H_{33} + \\ + \sigma_0 \sigma_0' H_{34} + \sigma_0'^2 H_{44} , \quad (32) \end{aligned}$$

where

$$\begin{aligned} H_0 = \frac{F_{10}^2}{k_1^4} \left(\frac{F_{30}}{k_1^2} - \frac{1}{2} \right) \sin^2 k_1 \phi - \frac{F_{10}^2}{k_1^4} \left(\frac{3F_{30}}{k_1^2} - \frac{1}{2} \right) k_1 \phi \sin k_1 \phi + \\ + \frac{F_{10}}{k_1^2} \left(1 + \frac{4F_{10} F_{30}}{k_1^4} \right) (1 - \cos k_1 \phi) , \end{aligned}$$

$$\begin{aligned} H_1 = \frac{F_{10}}{k_1^2} \left(1 - \frac{2F_{30}}{k_1^2} \right) \sin^2 k_1 \phi + \frac{F_{10}}{k_1^2} \left(\frac{3F_{30}}{k_1^2} - \frac{1}{2} \right) k_1 \phi \sin k_1 \phi + \\ + \left(1 + \frac{2F_{10} F_{30}}{k_1^4} \right) \cos k_1 \phi - \frac{2F_{10} F_{30}}{k_1^4} , \end{aligned}$$

$$\begin{aligned}
H_2 &= \frac{F_{10}}{k_1^3} \left(\frac{2F_{30}}{k_1^2} - 1 \right) \sin k_1 \phi \cos k_1 \phi + \frac{F_{10}}{k_1^3} \left(\frac{1}{2} - \frac{3F_{30}}{k_1^2} \right) k_1 \phi \cos k_1 \phi + \\
&\quad + \frac{1}{k_1} \left(1 + \frac{F_{10}}{2k_1^2} + \frac{F_{10} F_{30}}{k_1^4} \right) \sin k_1 \phi , \\
H_{11} &= \left(\frac{F_{30}}{k_1^2} - \frac{1}{2} \right) \sin^2 k_1 \phi + \frac{F_{30}}{k_1^2} (1 - \cos k_1 \phi) , \\
H_{12} &= \frac{1}{k_1} \left(1 - \frac{2F_{30}}{k_1^2} \right) (\sin k_1 \phi \cos k_1 \phi - \sin k_1 \phi) , \\
H_{22} &= \frac{1}{k_1^2} \left(\frac{F_{30}}{k_1^2} - \frac{1}{2} \right) \cos^2 k_1 \phi - \frac{1}{k_1^2} \left(\frac{2F_{30}}{k_1^2} - \frac{1}{2} \right) \cos k_1 \phi + \frac{F_{30}}{k_1^4} , \\
H_{33} &= \frac{1}{2k_1^2} \left(F_{12} - \frac{1}{2} k_2^2 \right) (1 - \cos k_1 \phi) - \frac{F_{12} + \frac{1}{2} k_2^2}{2(4k_2^2 - k_1^2)} (\cos 2k_2 \phi - \cos k_1 \phi) , \\
H_{34} &= \frac{2}{k_2(4k_2^2 - k_1^2)} \left(\frac{k_2}{k_1} \sin k_1 \phi - \frac{1}{2} \sin 2k_2 \phi \right) \left(F_{12} + \frac{1}{2} k_2^2 \right) , \\
H_{44} &= \frac{1}{2k_2^2} \left[\frac{1}{k_1^2} \left(F_{12} - \frac{1}{2} k_2^2 \right) (1 - \cos k_1 \phi) - \frac{F_{12} + \frac{1}{2} k_2^2}{4k_2^2 - k_1^2} (\cos k_1 \phi - \cos 2k_2 \phi) \right]
\end{aligned}$$

If one restricts the solution to the median plane, terms in σ_0 and σ_0' do not appear and (32) reduces to the results recently published by Tasman and Boerboom.³⁷

Now we suppose all ions are of charge q_0 , but we allow a small momentum spread given by

$$p = p_0(1 + \beta) , \quad (33)$$

where β is small – of first order.

Then

$$\eta = \left(\frac{q_0}{2mV} \right)^{1/2} = \frac{q_0}{p} = \frac{\eta_0}{1 + \beta} , \quad (34)$$

³⁷H. A. Tasman and A. J. H. Boerboom, *Z. Naturforsch.* 14a, 121 (1959).

where, from (23), $\eta_0 r_0 B_0 = 1$. It then follows from (22) that

$$\left. \begin{aligned} k_1^2 &= -2F_{20} = \frac{1-n}{1+\beta}, & k_2^2 &= -2F_{02} = \frac{n}{1+\beta}, \\ \frac{F_{10}}{k_1^2} &= \frac{\beta}{1-n}, & \frac{F_{30}}{k_1^2} &= \frac{n-b}{3(1-n)} = \frac{X}{6}, \\ F_{12} &= -\frac{(n/2)-b}{1+\beta} = \frac{n-X(1-n)}{2(1+\beta)}, \end{aligned} \right\} \quad (35)$$

where

$$X \equiv \frac{2(n-b)}{1-n}. \quad (36)$$

With the aid of these equations the second-order approximation for the radial coordinate of the ion trajectories (32) now becomes

$$\begin{aligned} \rho(\phi) &= \rho_0 D_1 + \rho_0' D_2 + \beta D_3 + \rho_0^2 D_{11} + \rho_0 \rho_0' D_{12} + \rho_0 \beta D_{13} + \rho_0'^2 D_{22} + \\ &\quad + \rho_0' \beta D_{23} + \beta^2 D_{33} + \sigma_0^2 D_{44} + \sigma_0 \sigma_0' D_{45} + \sigma_0'^2 D_{55}, \end{aligned} \quad (37)$$

where

$$D_1 = \cos k_1 \phi, \quad D_2 = (1-n)^{-1/2} \sin k_1 \phi, \quad D_3 = (1-n)^{-1} (1 - \cos k_1 \phi),$$

$$D_{11} = \frac{1}{6} [(X-3) \sin^2 k_1 \phi + X(1 - \cos k_1 \phi)],$$

$$D_{12} = \frac{1}{3} (1-n)^{-1/2} (3-X) (\sin k_1 \phi \cos k_1 \phi - \sin k_1 \phi),$$

$$\begin{aligned} D_{13} &= \frac{1}{6(1-n)} [2(3-X) \sin^2 k_1 \phi + 3(X-1)(1-n)^{1/2} \phi \sin k_1 \phi - \\ &\quad - 2X(1 - \cos k_1 \phi)], \end{aligned}$$

$$D_{22} = \frac{1}{6(1-n)} [(X-3) \cos^2 k_1 \phi - 2(X-3) \cos k_1 \phi + X],$$

$$\begin{aligned} D_{23} &= \frac{1}{6(1-n)^{3/2}} [2(X-3) \sin k_1 \phi \cos k_1 \phi - 3(X-1)(1-n)^{1/2} \phi \cos k_1 \phi + \\ &\quad + (6-3n+X) \sin k_1 \phi], \end{aligned}$$

$$\begin{aligned} D_{33} &= \frac{1}{6(1-n)^2} [(X-3) \sin^2 k_1 \phi - 3(X-1)(1-n)^{1/2} \phi \sin k_1 \phi + \\ &\quad + 4X(1 - \cos k_1 \phi)], \end{aligned}$$

$$\begin{aligned}
D_{44} &= -\frac{X}{4}(1 - \cos k_1 \phi) - \frac{b}{2(5n-1)}(\cos 2k_2 \phi - \cos k_1 \phi) , \\
D_{45} &= \frac{2b}{5n-1} \left[\frac{1}{(1-n)^{1/2}} \sin k_1 \phi - \frac{1}{2n^{1/2}} \sin 2k_2 \phi \right] , \\
D_{55} &= -\frac{1}{2n} \left[\frac{b}{5n-1}(\cos k_1 \phi - \cos 2k_2 \phi) + \frac{X}{2}(1 - \cos k_1 \phi) \right] .
\end{aligned} \tag{38}$$

If we omit the D_{44} , D_{45} , and D_{55} terms in Eq. (37), the solution reduces to the orbit in the median plane and then corresponds to Tasman's result.³⁷ The D_{13} , D_{23} , and D_{33} terms differ slightly from the corresponding terms in Tasman's equation, and it appears that the latter results are in error.

Solution to Axial Equation. – Following the same procedure as that presented above, the solution to the axial equation of motion (29), for ions of momentum p_0 , is

$$\sigma = \sigma_0 E_4 + \sigma_0' E_5 + \rho_0 \sigma_0 E_{14} + \rho_0' \sigma_0 E_{24} + \rho_0 \sigma_0' E_{15} + \rho_0' \sigma_0' E_{25} , \tag{39}$$

where

$$\begin{aligned}
k_1 &= (1-n)^{1/2} , & k_2 &= n^{1/2} , \\
E_4 &= \cos k_2 \phi , & E_5 &= \frac{1}{k_2} \sin k_2 \phi ,
\end{aligned}$$

$$\begin{aligned}
E_{14} &= -\frac{n}{5n-1} \sin k_2 \phi - \frac{n+2b}{5n-1} \cos k_2 \phi + \frac{1}{2} \cos k_1 \phi \cos k_2 \phi + \\
&+ \frac{1}{2} \frac{k_2}{k_1} \sin k_1 \phi \cos k_2 \phi - \frac{n-2b}{2k_1 k_2} \sin k_1 \phi \sin k_2 \phi + \\
&+ \frac{k_1 k_2 - (n-2b)}{4k_2(2k_2 - k_1)} \cos(k_2 - k_1) \phi - \frac{k_1 k_2 + (n-2b)}{4k_2(2k_2 + k_1)} \cos(k_1 + k_2) \phi - \\
&- \frac{k_2}{4(2k_2 - k_1)} \sin(k_2 - k_1) \phi - \frac{k_2}{4(2k_2 + k_1)} \sin(k_2 + k_1) \phi ,
\end{aligned}$$

$$\begin{aligned}
E_{24} = & \frac{k_2}{2} \left(\frac{5n}{5n-1} \right) \cos k_2 \phi - \frac{2[n(n-3b)+b]}{k_2(1-n)(5n-1)} \sin k_2 \phi + \frac{n-2b}{2k_1^2 k_2} \cos k_1 \phi \sin k_2 \phi - \\
& - \frac{k_2}{2} \cos k_1 \phi \cos k_2 \phi + \frac{1}{2k_1} \sin k_1 \phi \cos k_2 \phi - \frac{k_2}{4k_1(2k_2-k_1)} \cos(k_2-k_1)\phi + \\
& + \frac{k_2}{4k_1(2k_2+k_1)} \cos(k_2+k_1)\phi + \frac{(n-2b)-k_1 k_2}{4k_1 k_2(2k_2-k_1)} \sin(k_2-k_1)\phi - \\
& - \frac{(n-2b)+k_1 k_2}{4k_1 k_2(2k_2+k_1)} \sin(k_2+k_1)\phi ,
\end{aligned}$$

$$\begin{aligned}
E_{15} = & \frac{k_2}{5n-1} \cos k_2 \phi - \frac{6(n-b)-1}{k_2(5n-1)} \sin k_2 \phi - \frac{1}{2k_1} \sin k_1 \phi \sin k_2 \phi + \\
& + \frac{1}{2k_2} \cos k_1 \phi \sin k_2 \phi + \frac{n-2b}{2k_1 k_2^2} \sin k_1 \phi \cos k_2 \phi - \frac{1}{4(2k_2-k_1)} \cos(k_2-k_1)\phi - \\
& - \frac{1}{4(2k_2+k_1)} \cos(k_2+k_1)\phi + \frac{k_1 k_2 - (n-2b)}{4k_2^2(2k_2-k_1)} \sin(k_2-k_1)\phi - \\
& - \frac{k_1 k_2 + (n-2b)}{4k_2^2(2k_2+k_1)} \sin(k_2+k_1)\phi ,
\end{aligned}$$

$$\begin{aligned}
E_{25} = & - \frac{3n-1}{(1-n)(5n-1)} \sin k_2 \phi - \frac{1-3n+4b}{(1-n)(5n-1)} \cos k_2 \phi + \frac{1}{2k_1 k_2} \sin k_1 \phi \sin k_2 \phi + \\
& + \frac{1}{2k_1^2} \cos k_1 \phi \sin k_2 \phi - \frac{n-2b}{2k_1^2 k_2^2} \cos k_1 \phi \cos k_2 \phi + \\
& + \frac{1}{4k_1(2k_2-k_1)} \sin(k_2-k_1)\phi - \frac{1}{4k_1(2k_2+k_1)} \sin(k_2+k_1)\phi + \\
& + \frac{k_1 k_2 - (n-2b)}{4k_1 k_2^2(2k_2-k_1)} \cos(k_2-k_1)\phi + \frac{k_1 k_2 + (n-2b)}{4k_1 k_2^2(2k_2+k_1)} \cos(k_2+k_1)\phi .
\end{aligned}$$

5. ION TRAJECTORIES IN FIELD-FREE IMAGE SPACE

Neglecting fringing effects for the moment, we assume the field to exist only in the sector-shaped region between the circular boundaries whose radii of curvature are R_1 and R_2 . When the field boundary is concave inward, R_1 and R_2 are defined as positive. The sector field is

that

$$\rho_0 = \frac{1}{r_0} (l_o \alpha_r + \delta y) \quad \text{and} \quad \sigma_0 = \frac{1}{r_0} (l_o \alpha_z + \delta z) . \quad (40)$$

Through second-order approximation, the curved field boundary affects only the slope of the ion trajectories in the radial plane as they enter and leave the field. Then from Fig. 2,

$$\alpha_r \approx \tan \alpha_r = \left[\frac{1}{r} \frac{dr}{d\phi} - \theta_1 \right]_{\phi=0} = \left[\frac{1}{1+\rho} \frac{d\rho}{d\phi} - \theta_1 \right]_{\phi=0} ,$$

where $\theta_1 = b_1/r_0 \approx (\rho r_0)^2/2r_0 R_1|_{\phi=0}$. Hence,

$$\rho'_0 = (1+\rho_0)(\alpha_r + \theta_1) \approx \alpha_r + \frac{l_o}{r_0} \left(1 + \frac{l_o}{2R_1} \right) \alpha_r^2 + \frac{1}{r_0} \left(1 + \frac{l_o}{R_1} \right) \alpha_r \delta y + \frac{(\delta y)^2}{2R_1 r_0} . \quad (41)$$

Also,

$$\alpha_z \approx \tan \alpha_z = \frac{1}{r} \frac{dz}{d\phi} \Big|_{\phi=0} = \sigma'_0 . \quad (42)$$

In the field-free image space we may express the rectilinear ion path in terms of the Cartesian coordinates x, y, z defined in Fig. 2. Thus in the midplane,

$$y = \left[y + x \frac{dy}{dx} \right]_{x=0} \approx \left[r_0 \rho + x \left(\frac{1}{r} \frac{dr}{d\phi} + \theta_2 \right) \right]_{\phi=\Phi} .$$

Now $\theta_2 = b_2/r_0 \approx r_0 \rho^2/2R_2|_{\phi=\Phi}$, and so

$$y = \left\{ r_0 \rho + x \left[(1 - \rho + \rho^2 - \dots) \frac{d\rho}{d\phi} + \frac{r_0 \rho^2}{2R_2} \right] \right\}_{\phi=\Phi} . \quad (43)$$

Then with the aid of Eqs. (37), (38), (40), (41), and (42) we may write this last equation in the form

$$\begin{aligned} y = r_0 [& M_1 \alpha_r + M_2 \beta + M_3 \delta y + M_{11} \alpha_r^2 + M_{12} \alpha_r \beta + M_{13} \alpha_r \delta y + M_{22} \beta^2 + M_{23} \beta \delta y + \\ & + M_{33} (\delta y)^2 + M_{44} \alpha_z^2 + M_{45} \alpha_z \delta z + M_{55} (\delta z)^2] + x [N_1 \alpha_r + N_2 \beta + N_3 \delta y + \\ & + N_{11} \alpha_r^2 + N_{12} \alpha_r \beta + N_{13} \alpha_r \delta y + N_{22} \beta^2 + N_{23} \beta \delta y + N_{33} (\delta y)^2 + \\ & + N_{44} \alpha_z^2 + N_{45} \alpha_z \delta z + N_{55} (\delta z)^2] , \quad (44) \end{aligned}$$

where

$$\left. \begin{aligned}
 M_1 &= \frac{l_o}{r_0} D_1 + D_2, & M_2 &= D_3, & M_3 &= \frac{D_1}{r_0}, \\
 M_{11} &= \left[\frac{l_o}{r_0} \left(1 + \frac{l_o}{2R_1} \right) D_2 + \frac{l_o^2}{r_0^2} D_{11} + \frac{l_o}{r_0} D_{12} + D_{22} \right], & M_{12} &= \frac{l_o}{r_0} D_{13} + D_{23}, \\
 M_{13} &= \left[\frac{1}{r_0} \left(1 + \frac{l_o}{R_1} \right) D_2 + \frac{2l_o}{r_0^2} D_{11} + \frac{D_{12}}{r_0} \right], & M_{22} &= D_{33}, & M_{23} &= \frac{D_{13}}{r_0}, \\
 M_{33} &= \left(\frac{D_2}{2R_1 r_0} + \frac{D_{11}}{r_0^2} \right), & M_{44} &= \frac{l_o^2}{r_0^2} D_{44} + \frac{l_o}{r_0} D_{45} + D_{55}, \\
 M_{45} &= \frac{2l_o}{r_0} D_{44} + \frac{D_{45}}{r_0}, & M_{55} &= \frac{D_{44}}{r_0^2},
 \end{aligned} \right\} (45)$$

and

$$\begin{aligned}
 N_1 &= \frac{l_o}{r_0} D'_1 + D'_2, & N_2 &= D'_3, & N_3 &= \frac{D'_1}{r_0}, \\
 N_{11} &= \frac{l_o}{r_0} D'_2 + \frac{l_o^2}{r_0^2} D'_{11} + \frac{l_o}{r_0} D'_{12} + D'_{22} - D_1 \left(\frac{l_o^2}{r_0^2} D'_1 + \frac{l_o}{r_0} D'_2 \right) - \\
 &\quad - D_2 \left(\frac{l_o}{r_0} D'_1 + D'_2 \right) + \frac{l_o^2}{2r_0 R_1} D'_2 + \frac{r_0}{2R_2} \left(\frac{l_o}{r_0} D_1 + D_2 \right)^2, \\
 N_{12} &= \frac{l_o}{r_0} D'_{13} + D'_{23} - D'_3 \left(\frac{l_o}{r_0} D_1 + D_2 \right) - D_3 \left(\frac{l_o}{r_0} D'_1 + D'_2 \right) + \\
 &\quad + \frac{1}{2} \left[\frac{l_o}{r_0} (1-n) D_2 - D_1 \right] + \frac{r_0}{R_2} \left(\frac{l_o}{r_0} D_1 D_3 + D_2 D_3 \right), \\
 N_{13} &= \frac{2l_o}{r_0} D'_{11} + \frac{1}{r_0} D'_{12} - \frac{2l_o}{r_0} D_1 D'_1 + \frac{1}{r_0} \left(1 + \frac{l_o}{R_1} \right) D'_2 + \frac{1}{R_2} (l_o D_1^2 + D_1 D_2), \\
 N_{22} &= D'_{33} - D_3 D'_3 - \frac{1}{2} D_2 + \frac{r_0}{2R_2} D_3^2, & N_{23} &= -\frac{1}{r_0} (D_1 D'_3 + D'_1 D_3) + \frac{1}{R_2} D_1 D_3, \\
 N_{33} &= \frac{1}{r_0^2} (D'_{11} - D_1 D'_1) + \frac{1}{2r_0} \left(\frac{D'_2}{R_1} + \frac{D_1'^2}{R_2} \right),
 \end{aligned}$$

$$N_{44} = \frac{l_o^2}{r_0^2} D'_{44} + \frac{l_o}{r_0} D'_{45} + D'_{55} ,$$

$$N_{45} = \frac{1}{r_0} (2l_o D'_{44} + D'_{45}) , \quad N_{55} = \frac{D'_{44}}{r_0^2} .$$

In these equations for the M 's and N 's, the D 's and their derivatives are to be evaluated at $\phi = \Phi$. The D functions are given by (38).

Following a similar procedure one may show that in the image space the trajectories in the vertical plane, for ions of momentum p_0 , are

$$z = r_0 (l_4 \alpha_z + l_5 \delta z + l_{14} \alpha_r \alpha_z + l_{15} \alpha_r \delta z + l_{34} \delta y \alpha_z + l_{35} \delta y \delta z) + \\ + x (J_4 \alpha_z + J_5 \delta z + J_{14} \alpha_r \alpha_z + J_{15} \alpha_r \delta z + J_{34} \alpha_z \delta y + J_{35} \delta y \delta z) , \quad (46)$$

where (all functions to be evaluated at $\phi = \Phi$)

$$l_4 = \frac{l_o}{r_0} E_4 + E_5 , \quad l_5 = \frac{E_4}{r_0} ,$$

$$l_{14} = \frac{l_o^2}{r_0^2} E_{14} + \frac{l_o}{r_0} E_{24} + \frac{l_o}{r_0} E_{15} + E_{25} ,$$

$$l_{15} = \frac{l_o}{r_0^2} E_{14} + \frac{1}{r_0} E_{24} ,$$

$$l_{34} = \frac{l_o}{r_0^2} E_{14} + \frac{1}{r_0} E_{15} ,$$

$$l_{35} = \frac{1}{r_0^2} E_{14} ,$$

and

$$J_4 = \frac{l_o}{r_0} E'_4 + E'_5 , \quad J_5 = \frac{1}{r_0} E'_4 ,$$

$$J_{14} = \frac{l_o^2}{r_0^2} (E'_{14} - D_1 E'_4) + \frac{l_o}{r_0} (E'_{24} - D_2 E'_4) + \frac{l_o}{r_0} (E'_{15} - D_1 E'_5) + (E'_{25} - D_2 E'_5) ,$$

$$J_{15} = \frac{l_o}{r_0^2} (E'_{14} - D_1 E'_4) + \frac{1}{r_0} (E'_{24} - D_2 E'_4) ,$$

$$J_{34} = \frac{l_o}{r_0^2} (E'_{14} - D_1 E'_4) + \frac{1}{r_0} (E'_{15} - D_1 E'_5) ,$$

$$J_{35} = \frac{1}{r_0^2} (E'_{14} - D_1 E'_4) .$$

The D and E functions are given by (38) and (39), respectively.

6. IMAGE PROPERTIES

Focal Distances

First-order radial focusing occurs at the position where the term proportional to α_r in Eq. (44) vanishes. Thus, ions of momentum p_0 ($\beta = 0$) focus in the radial plane at the image distance

$$l_r = -r_0 \frac{M_1}{N_1} .$$

Evaluating the functions M_1 and N_1 from (45) and (38), this last equation becomes

$$l_r = -\frac{r_0}{(1-n)^{1/2}} \tan \left[(1-n)^{1/2} \Phi + \tan^{-1} \frac{l_o}{r_0} (1-n)^{1/2} \right] . \quad (47)$$

Similar considerations lead to the first-order vertical focusing condition, namely,

$$l_z = -\frac{r_0}{n^{1/2}} \tan \left(n^{1/2} \Phi + \tan^{-1} \frac{l_o}{r_0} n^{1/2} \right) . \quad (48)$$

These conditions for radial and vertical focusing have a very useful geometric interpretation.

Let

$$a_r + b_r + c_r = \pi .$$

Then

$$\tan(a_r + b_r) = \tan(\pi - c_r) = -\tan c_r , \quad (49)$$

and comparing (49) with (47) one can make the identifications

$$a_r = (1-n)^{1/2} \Phi , \quad b_r = \tan^{-1} \frac{l_o}{r_0} (1-n)^{1/2} , \quad c_r = \tan^{-1} \frac{l_r}{r_0} (1-n)^{1/2} .$$

The radial focus condition can then be written as

$$(1-n)^{1/2} \Phi + \tan^{-1} \frac{l_o}{r_0} (1-n)^{1/2} + \tan^{-1} \frac{l_r}{r_0} (1-n)^{1/2} = \pi , \quad (50)$$

and similarly for the vertical motion

$$n^{1/2} \Phi + \tan^{-1} \frac{L_o}{r_o} n^{1/2} + \tan^{-1} \frac{L_z}{r_o} n^{1/2} = \pi . \quad (51)$$

A geometric interpretation of these last two equations is illustrated in Fig. 3.

Magnification

The lateral magnification M_r is defined as the ratio of the image width at the radial focus position to the object width and is assumed to be positive if the image is inverted. It follows

UNCLASSIFIED
ORNL-LR-DWG 45142

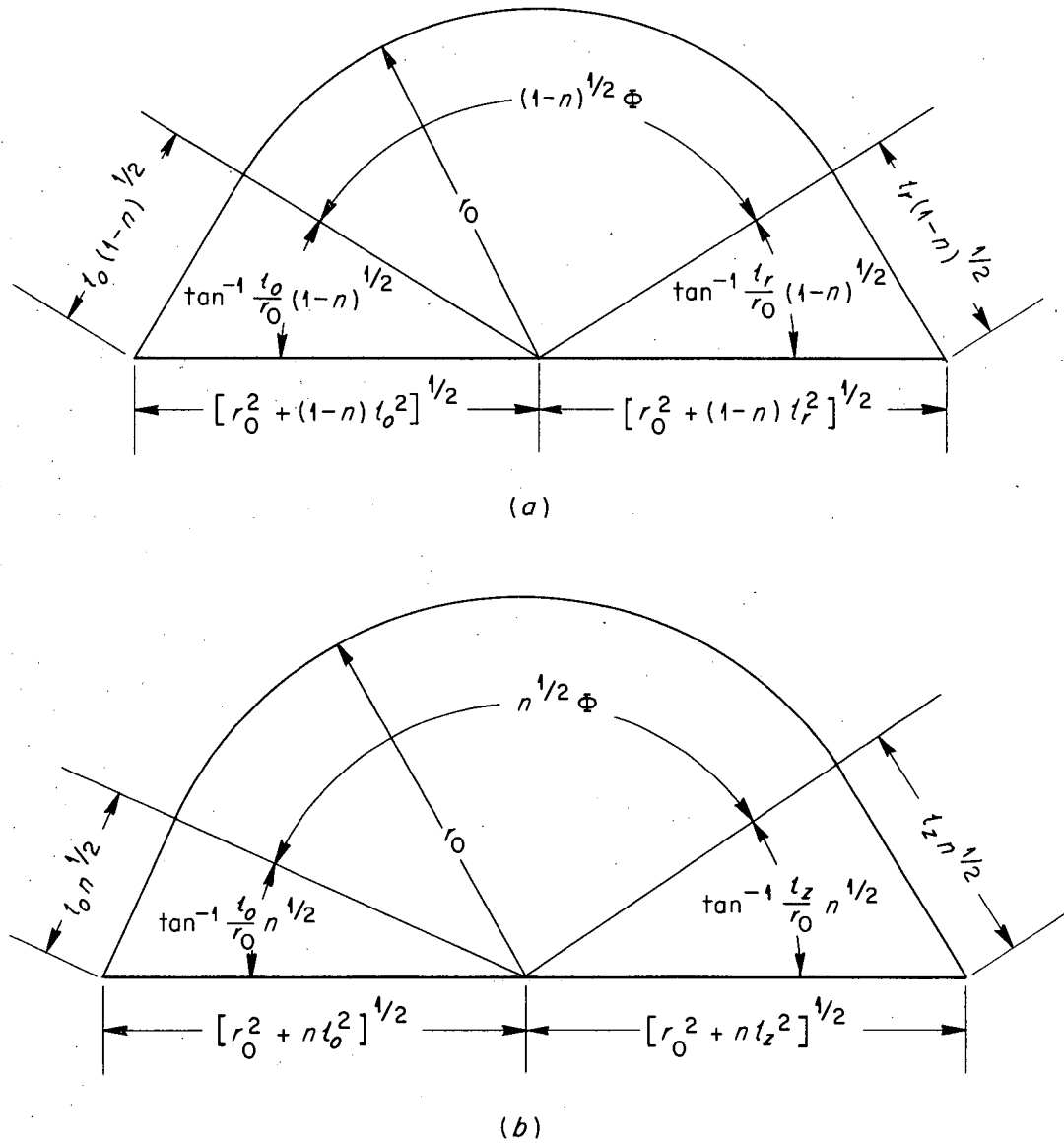


Fig. 3. Geometric Interpretation of Focus Conditions. (a) Radial focusing; (b) vertical focusing.

directly from Eq. (44) that, for ions of the same momentum ($\beta = 0$),

$$M_r = -(r_0 M_3 + l_r N_3) ,$$

which from (45) and (47) becomes

$$\begin{aligned} M_r &= (1-n)^{1/2} \frac{l_r}{r_0} \sin(1-n)^{1/2} \Phi - \cos(1-n)^{1/2} \Phi \\ &= \left[(1-n)^{1/2} \frac{l_o}{r_0} \sin(1-n)^{1/2} \Phi - \cos(1-n)^{1/2} \Phi \right]^{-1} . \end{aligned} \quad (52)$$

The vertical magnification M_z is defined as the ratio of the image height to the object height measured normal to the $z = 0$ plane. Like M_r , M_z is taken to be positive if the image is inverted with respect to the object. Using the same method as above, but applied to the vertical motion of the ions, one may show that

$$M_z = n^{1/2} \frac{l_z}{r_0} \sin n^{1/2} \Phi - \cos n^{1/2} \Phi . \quad (53)$$

Mass Dispersion

Suppose all ions are of the same energy qV but a small mass difference δm is allowed. Then

$$\eta \equiv \left(\frac{q}{2mV} \right)^{1/2} = \left\{ \frac{q}{2m_0 V [1 + (\delta m/m_0)]} \right\}^{1/2} = \eta_0 \left(1 + \frac{1}{2} \frac{\delta m}{m_0} + \dots \right)^{-1} ,$$

and from (34) we see that in first-order approximation

$$\beta = \frac{1}{2} \frac{\delta m}{m_0} . \quad (54)$$

For a monoenergetic ion beam of mass $m_0 + \delta m$ the lateral displacement D in the y direction at the image position l_r is given by the sum of terms proportional to β in (44). Hence,

$$D = \beta(r_0 M_2 + l_r N_2) ,$$

which from (45) and (54) becomes

$$\begin{aligned} D &= \frac{\delta m}{2m_0(1-n)} \left\{ r_0 [1 - \cos(1-n)^{1/2} \Phi] + l_r (1-n)^{1/2} \sin(1-n)^{1/2} \Phi \right\} \\ &= \frac{r_0}{1-n} \frac{\delta m}{2m_0} (1 + M_r) , \end{aligned} \quad (55)$$

where M_r is the lateral magnification. This is a measure of the mass dispersion D_m defined as

$$D_m = \frac{D}{\delta m/m_0} = \frac{1}{2} \frac{r_0}{1-n} (1 + M_r) . \quad (56)$$

In general, the focusing plane of the mass spectrum is not perpendicular to the central ion path, since the image distance depends on β and hence on $m = m_0 + \delta m$. From Eqs. (44) and (54) we see that ions of mass $m_0 + \delta m$ produce an image at

$$l_r(\beta) = \frac{r_0 \left[M_1 + \frac{1}{2} (\delta m/m_0) M_{12} \right]}{N_1 + \frac{1}{2} (\delta m/m_0) N_{12}} \quad (57)$$

Chromatic Aberration

We now suppose all ions are of the same mass m_0 , but we allow a small energy spread $q \delta V$. This energy spread arises from the fact that the ion possesses a small amount of energy before being accelerated by the potential difference V . Hence,

$$\eta = \left\{ \frac{q}{2m_0 V [1 + (\delta V/V)]} \right\}^{1/2} = \eta_0 \left(1 + \frac{1}{2} \frac{\delta V}{V} + \dots \right)^{-1},$$

and again from (34) it follows that

$$\beta = \frac{1}{2} \frac{\delta V}{V} \quad (58)$$

The lateral displacement D_E at the focus position l_r due to ions of energy $q(V + \delta V)$ must be the same as that given in the previous paragraph with $\delta m/m_0$ replaced by $\delta V/V$. The chromatic aberration may then be written as

$$D_E = \frac{r_0}{1-n} \frac{\delta V}{2V} (1 + M_r) \quad (59)$$

This term may be minimized in the usual manner – through the use of large accelerating potentials V or by an electrostatic energy filter.

Solid Angle

According to Judd,³⁸ the solid angle Ω (in steradians) for such an inhomogeneous magnetic analyzer is given by

$$\frac{\Omega}{A} = \left[\left(\frac{l_o}{r_0} \right)^4 + \frac{1 + (l_o/r_0)^2}{n(1-n)} \right]^{-1/2} \quad (60)$$

where $A r_0^2$ is the maximum available cross-sectional area for the ion path. This formula assumes that $A r_0^2$ is independent of ϕ and that l_r and $l_z \leq \infty$, corresponding to converging or parallel outgoing beams.

³⁸D. L. Judd, *Rev. Sci. Instr.* **21**, 213 (1950).

Second-Order Radial Aberration

If all ions are of the same mass m_0 , the total image width at the radial focus position is limited by second-order radial aberration terms. The image width is given by Eq. (44) evaluated at $x = l_r$. Thus with β given by (58),

$$\begin{aligned}
 y(x = l_r) = & -M_r \delta y + D_E + r_0 \left[\alpha_r^2 \left(M_{11} + \frac{l_r}{r_0} N_{11} \right) + \alpha_r \beta \left(M_{12} + \frac{l_r}{r_0} N_{12} \right) + \right. \\
 & + \alpha_r \delta y \left(M_{13} + \frac{l_r}{r_0} N_{13} \right) + \beta^2 \left(M_{22} + \frac{l_r}{r_0} N_{22} \right) + \\
 & + \beta \delta y \left(M_{23} + \frac{l_r}{r_0} N_{23} \right) + (\delta y)^2 \left(M_{33} + \frac{l_r}{r_0} N_{33} \right) + \\
 & \left. + \alpha_z^2 \left(M_{44} + \frac{l_r}{r_0} N_{44} \right) + \alpha_z \delta z \left(M_{45} + \frac{l_r}{r_0} N_{45} \right) + (\delta z)^2 \left(M_{55} + \frac{l_r}{r_0} N_{55} \right) \right]. \quad (61)
 \end{aligned}$$

Second-order terms containing the object width δy may be neglected, since the presence of the first-order term in (61) requires δy to be extremely small. Similarly, the second-order energy aberration term, proportional to β^2 , and the mixed term proportional to $\alpha_r \beta$ must be negligibly small. It is convenient to rewrite this last equation as follows:

$$y(l_r) = -M_r \delta y + \frac{r_0}{1-n} (1 + M_r) \frac{\delta V}{2V} + A_{11} \alpha_r^2 + \dots + A_{44} \alpha_z^2 + A_{45} \alpha_z \delta z + A_{55} (\delta z)^2, \quad (62)$$

where the A 's have the obvious meaning from (61).

The explicit form of the angular aberration term A_{11} may be found from (45) and (38). Thus

$$A_{11} = r_0 \left(M_{11} + \frac{l_r}{r_0} N_{11} \right), \quad (63)$$

where [by defining $\Phi_r \equiv (1-n)^{1/2} \Phi$]

$$\begin{aligned}
 M_{11} = & \frac{1}{6(1-n)} [(X-3) \cos^2 \Phi_r - (2X-3) \cos \Phi_r + X] + \\
 & + \frac{l_0}{3r_0(1-n)^{1/2}} [X \sin \Phi_r - (X-3) \sin \Phi_r \cos \Phi_r] + \\
 & + \frac{l_0^2}{6r_0^2} [X(1 - \cos \Phi_r) + (X-3) \sin^2 \Phi_r] + \frac{l_0^2 \sin \Phi_r}{2r_0 R_1 (1-n)^{1/2}},
 \end{aligned}$$

$$\begin{aligned}
N_{11} = & \frac{1}{6(1-n)^{1/2}} [-2X \sin \Phi_r \cos \Phi_r + (2X-3) \sin \Phi_r] + \\
& + \frac{l_o X}{3r_0} (2 \sin^2 \Phi_r + \cos \Phi_r - 1) + \frac{l_o^2}{2r_0 R_1} \cos \Phi_r + \\
& + \frac{l_o^2 (1-n)^{1/2} X}{6r_0^2} (2 \sin \Phi_r \cos \Phi_r + \sin \Phi_r) + \\
& + \frac{r_0}{2R_2} \left[\frac{l_o}{r_0} \cos \Phi_r + (1-n)^{-1/2} \sin \Phi_r \right]^2 .
\end{aligned}$$

This result agrees with the second-order angular aberration term given by Tasman³⁹ for the case $R_1 = R_2 = \infty$. We may eliminate the angle Φ from (63) by making use of the focus condition (50). Letting

$$\begin{aligned}
l'_o & \equiv \frac{l_o}{r_0} (1-n)^{1/2} , & l'_r & \equiv \frac{l_r}{r_0} (1-n)^{1/2} , & R'_1 & \equiv (1-n)^{1/2} \frac{R_1}{r_0} , \\
R'_2 & \equiv (1-n)^{1/2} \frac{R_2}{r_0} , & t_0 & \equiv (1+l_o'^2)^{1/2} , & t_1 & \equiv (1+l_r'^2)^{1/2} ,
\end{aligned} \tag{64}$$

we see from Fig. 3 that

$$\begin{aligned}
\sin \Phi_r & = \sin (\tan^{-1} l'_o + \tan^{-1} l'_r) = \frac{1}{t_0 t_1} (l'_o + l'_r) , \\
\cos \Phi_r & = -\cos (\tan^{-1} l'_o + \tan^{-1} l'_r) = \frac{1}{t_0 t_1} (l'_o l'_r - 1) .
\end{aligned} \tag{65}$$

Using (65) to eliminate Φ_r from (63) we obtain

$$A_{11} = -\frac{r_0}{2(1-n)} \left\{ \frac{t_1}{t_0} \left[1 - \frac{X}{3} (2 + 3l_o'^2) - \frac{l_o'^3}{R_1'} \right] + \frac{t_0^2}{t_1^2} \left[1 - \frac{X}{3} (2 + 3l_r'^2) - \frac{l_r'^3}{R_2'} \right] \right\} . \tag{66}$$

From Eqs. (38), (45), and (62) it follows that

$$\begin{aligned}
A_{44} = r_0 \left(M_{44} + \frac{l_r}{r_0} N_{44} \right) = -\frac{r_0}{n} \left[\frac{X}{4} (1 + M_r) \left(1 + \frac{nl_o^2}{r_0^2} \right) + K \left(1 - \frac{nl_o^2}{r_0^2} \right) + \right. \\
\left. + \frac{(1-n)^{1/2} l_o}{r_0} L \right] , \tag{67}
\end{aligned}$$

³⁹H. A. Tasman and A. J. H. Boerboom, *Z. Naturforsch.* 14a, 121 (1959).

$$A_{45} = r_0 \left(M_{45} + \frac{l_o}{r_0} N_{45} \right) = -\frac{1}{n^{1/2}} \left\{ \frac{n^{1/2} l_o}{r_0} \left[\frac{X}{2} (1 + M_r) - 2K \right] + L \right\}, \quad (68)$$

$$A_{55} = r_0 \left(M_{55} + \frac{l_r}{r_0} N_{55} \right) = -\frac{1}{r_0} \left[\frac{X}{4} (1 + M_r) - K \right], \quad (69)$$

where

$$K \equiv \frac{b}{2(5n-1)} \left(\frac{2n^{1/2} l_r}{r_0} \sin 2n^{1/2} \Phi - \cos 2n^{1/2} \Phi - M_r \right), \quad X \equiv \frac{2(n-b)}{1-n},$$

$$L \equiv \frac{b}{5n-1} \left(\frac{2n^{1/2} l_r}{r_0} \cos 2n^{1/2} \Phi + \sin 2n^{1/2} \Phi - \frac{2n^{1/2} l_o}{r_0} M_r \right).$$

These equations are in agreement with the recently published results of Ikegami.⁴⁰

Resolution

The mass resolving power R is defined as the reciprocal of the relative mass difference $\delta m/m_0$ required to move an image out of the collector slit so as not to be confused with an adjacent image. Therefore

$$R = \frac{D_m}{s_1 M_r + s_2 + \Sigma A} = \frac{r_0 (1 + M_r)}{2(1-n)(s_1 M_r + s_2 + \Sigma A)},$$

where s_1 and s_2 are the object and image slit widths, respectively, and ΣA is the total beam broadening due to all aberrations. Neglecting third- and higher-order aberrations as well as pressure broadening effects, the mass resolving power is given by

$$R = \frac{r_0 (1 + M_r)}{2(1-n) [s_1 M_r + s_2 + D_E + A_{11} \alpha_r^2 + A_{44} \alpha_z^2 + A_{45} \alpha_z \delta z + A_{55} (\delta z)^2]}. \quad (70)$$

As was seen in the last section, the $A_{11} \alpha_r^2$ term can be reduced to third order by shaping the pole boundaries and the remaining second-order terms minimized by a proper choice of the field constant b .

⁴⁰H. Ikegami, *Rev. Sci. Instr.* **29**, 943 (1958).

Vertical Aberration

The total beam height at the radial focus position is given by (46) evaluated at $x = l_r$. Thus for ions of momentum p_0 ,

$$z(l_r) = -M_z \delta z + r_0 \left[\alpha_z \left(l_4 + \frac{l_r}{r_0} J_4 \right) + \alpha_r \alpha_z \left(l_{14} + \frac{l_r}{r_0} J_{14} \right) + \alpha_r \delta z \left(l_{15} + \frac{l_r}{r_0} J_{15} \right) + \delta y \alpha_z \left(l_{34} + \frac{l_r}{r_0} J_{34} \right) + \delta y \delta z \left(l_{35} + \frac{l_r}{r_0} J_{35} \right) \right]. \quad (71)$$

Second-order vertical aberration terms become important only at the axial focus position l_z . The terms proportional to $\alpha_r \delta z$ and $\delta y \delta z$ are negligible because of the presence of the first-order term, $-M_z \delta z$. Terms making a significant contribution to the geometric aberration in the vertical plane are therefore

$$A_{14} \alpha_r \alpha_z \equiv r_0 \left(l_{14} + \frac{l_z}{r_0} J_{14} \right) \alpha_r \alpha_z, \quad (72)$$

$$A_{34} \delta y \alpha_z \equiv r_0 \left(l_{34} + \frac{l_z}{r_0} J_{34} \right) \delta y \alpha_z.$$

Note that through second order the total vertical aberration does not contain R_1 and R_2 and therefore is not affected by curving the entrance and exit boundaries of the field.

7. IMAGE PROPERTIES FOR AN INFLECTION SPECTROMETER

For the sake of completeness we now derive the image properties, in first order, for an ion beam entering and leaving the inhomogeneous magnetic sector field at arbitrary angles with respect to the normal to the pole edge. The equations of motion developed in Sec 4 are still applicable; however, the boundary conditions used in Sec 5 for the case of normal entry and exit must now be modified.

Radial Focusing, Magnification, and Mass Dispersion

As can be seen from Fig. 4,

$$\delta r|_{\phi=0} \approx \delta y + l_o \alpha_r \quad \text{and} \quad \gamma_1 \approx \frac{1}{r} \frac{dr}{d\phi} \Big|_{\phi=0} = \alpha_r + \beta_1 \approx \alpha_r + \frac{\delta r}{r_0} \Big|_{\phi=0} \tan \epsilon_1,$$

yielding the initial conditions

$$\rho_0 = \frac{1}{r_0} (l_o \alpha_r + \delta y), \quad (73)$$

$$\rho_0' = (1 + \rho_0) (\alpha_r + \rho_0 \tan \epsilon_1).$$

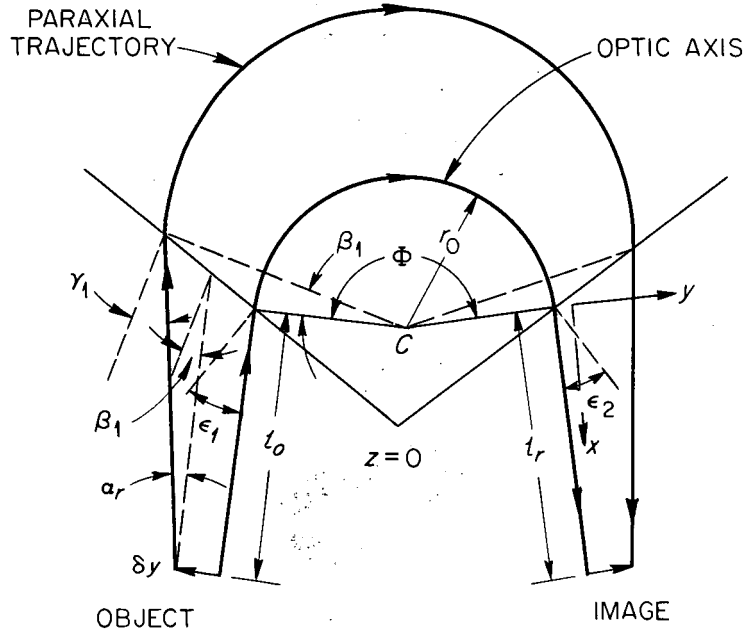


Fig. 4. Radial Focusing for Oblique Incidence.

In the field-free image space,

$$y = \left[y + x \frac{dy}{dx} \right]_{x=0} \approx \left[\delta r + x \left(\frac{1}{r} \frac{dr}{d\phi} + \frac{\delta r}{r_0} \tan \epsilon_2 \right) \right]_{\phi=\Phi}$$

$$= r_0 \rho + x [(1 - \rho + \rho^2 - \dots) \rho' + \rho \tan \epsilon_2]_{\phi=\Phi} \quad (74)$$

Restricting our attention to terms no higher than first order, this last equation may be written in the form

$$y = P_1 \alpha_r + P_2 \beta + P_3 \delta y + x [Q_1 \alpha_r + Q_2 \beta + Q_3 \delta y] \quad (75)$$

where the P and Q functions are to be evaluated from (37), (38), (73), and (74). The results are, with $\Phi_r \equiv (1 - n)^{1/2} \Phi$,

$$P_1 = r_0 \left[\frac{l_o}{r_0} \cos \Phi_r + \left(1 + \frac{l_o}{r_0} \tan \epsilon_1 \right) (1 - n)^{-1/2} \sin \Phi_r \right],$$

$$P_2 = r_0 (1 - n)^{-1} (1 - \cos \Phi_r),$$

$$P_3 = \cos \Phi_r + (1 - n)^{-1/2} \sin \Phi_r \tan \epsilon_1,$$

$$\begin{aligned}
Q_1 &= -\frac{l_o}{r_0} (1-n)^{1/2} \sin \Phi_r + \left(1 + \frac{l_o}{r_0} \tan \epsilon_1\right) \cos \Phi_r + \frac{l_o}{r_0} \cos \Phi_r \tan \epsilon_2 + \\
&\quad + \left(1 + \frac{l_o}{r_0} \tan \epsilon_1\right) (1-n)^{-1/2} \sin \Phi_r \tan \epsilon_2 , \\
Q_2 &= (1-n)^{-1/2} \sin \Phi_r + (1-n)^{-1} (1 - \cos \Phi_r) \tan \epsilon_2 , \\
Q_3 &= \frac{1}{r_0} [-(1-n)^{1/2} \sin \Phi_r + (\tan \epsilon_1 + \tan \epsilon_2) \cos \Phi_r + \\
&\quad + (1-n)^{-1/2} \sin \Phi_r \tan \epsilon_1 \tan \epsilon_2] .
\end{aligned} \tag{76}$$

Following the arguments presented in Sec 6, ions of momentum p_0 ($\beta = 0$) are focused at that position for which the coefficient of α_r vanishes. From (75) and (76)

$$l_r = -\frac{r_0 P_1}{Q_1} = \frac{r_0}{(1-n)^{1/2} \tan \{(1-n)^{1/2} \Phi - \tan^{-1} (1-n)^{-1/2} [(r_0/l_o) + \tan \epsilon_1]\} - \tan \epsilon_2} . \tag{77}$$

The lateral magnification of the image position is found from the negative of the coefficient of δy in (75). Thus

$$\begin{aligned}
M_r &= -(r_0 P_3 + l_r Q_3) = -[\cos (1-n)^{1/2} \Phi + (1-n)^{-1/2} \sin (1-n)^{1/2} \Phi \tan \epsilon_1] + \\
&\quad + \frac{l_r}{r_0} [(1-n)^{1/2} \sin (1-n)^{1/2} \Phi - (\tan \epsilon_1 + \tan \epsilon_2) \cos (1-n)^{1/2} \Phi - \\
&\quad - (1-n)^{-1/2} \sin (1-n)^{1/2} \Phi \tan \epsilon_1 \tan \epsilon_2] .
\end{aligned} \tag{78}$$

As was shown in Sec 6, the coefficient of β is related to the mass dispersion D_m . Again from (75) and (76)

$$\begin{aligned}
D_m &= \frac{1}{2} (r_0 P_2 + l_r Q_2) \\
&= \frac{r_0}{2(1-n)} \left(1 - \cos (1-n)^{1/2} \Phi + \right. \\
&\quad \left. + \frac{l_r}{r_0} \{(1-n)^{1/2} \sin (1-n)^{1/2} \Phi + [1 - \cos (1-n)^{1/2} \Phi] \tan \epsilon_2\} \right) .
\end{aligned} \tag{79}$$

Equations (77), (78), and (79) reduce to (47), (52), and (56), respectively, for the case $\epsilon_1 = \epsilon_2 = 0$.

Vertical Focusing

Were it not for the fringing field, the vertical focus condition for the case of nonnormal entry would be the same as that for normal incidence [Eq. (48)]. In the present case, however, the fringe field exerts an axial force on the ion beam which alters the equation for vertical focusing.

Suppose that within the fringing field B_z increases from zero to its maximum value between $x = -\Delta x$ and $x = 0$. As is shown in Fig. 5, the x axis is taken normal to the pole edge; Δx is of the order of one gap width.

UNCLASSIFIED
ORNL-LR-DWG 45144

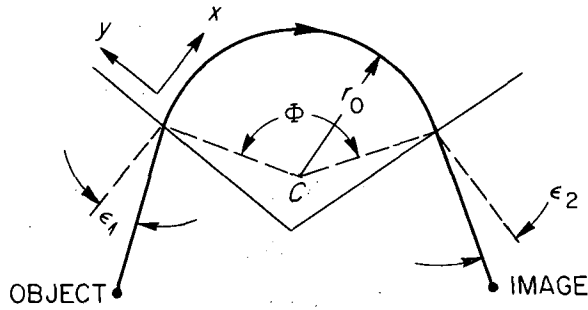


Fig. 5. Vertical Focusing for Oblique Incidence.

From the Maxwell equation $\nabla \times \mathbf{B} = 0$,

$$\frac{\partial B_x}{\partial z} - \frac{\partial B_z}{\partial x} = 0,$$

and so in the fringing field

$$B_x \approx z \left(\frac{B_z}{\Delta x} \right).$$

The z component of the magnetic force on the charged particle is

$$F_z = q(\mathbf{v} \times \mathbf{B})_z = -qv_y B_x = -qv(\sin \epsilon_1) B_x.$$

The time it takes the ion to cross Δx is

$$\Delta t = \frac{\Delta x}{v_x} = \frac{\Delta x}{v \cos \epsilon_1}.$$

Since force is the time rate of change of linear momentum,

$$\Delta p_z = F_z \Delta t = -qz B_z \tan \epsilon_1.$$

Within the sector field $p = qr_0 B_z$, and so

$$\frac{\Delta p_z}{p} = \frac{p_f - p_i}{p} = -\frac{z}{r_0} \tan \epsilon_1. \quad (80)$$

From Fig. 6 we see that

$$\frac{p_i}{p} = \tan \alpha_z \approx \frac{z}{l_o} \Big|_{\phi=0} = \frac{r_0}{l_o} \sigma_0, \quad \frac{p_f}{p} = \tan \psi = \frac{1}{r_0} \frac{dz}{d\phi} \Big|_{\phi=0} = \sigma'_0.$$

Equation (80) then becomes

$$\sigma'_0 = \sigma_0 \left(\frac{r_0}{l_o} - \tan \epsilon_1 \right). \quad (81)$$

An analogous equation applies at the exit, namely,

$$\sigma' \Big|_{\phi=\Phi} = -\sigma \left(\frac{r_0}{l_z} - \tan \epsilon_2 \right) \Big|_{\phi=\Phi}. \quad (82)$$

The vertical focus position l_z is now evaluated directly from (25), (81), and (82), with the result

$$l_z = \frac{r_0}{n^{1/2} \tan \{n^{1/2} \Phi - \tan^{-1} n^{-1/2} [(r_0/l_o) - \tan \epsilon_1]\} + \tan \epsilon_2}. \quad (83)$$

These focus conditions, (77) and (83), were first derived by Sternheimer.⁴¹

UNCLASSIFIED
ORNL-LR-DWG 45145

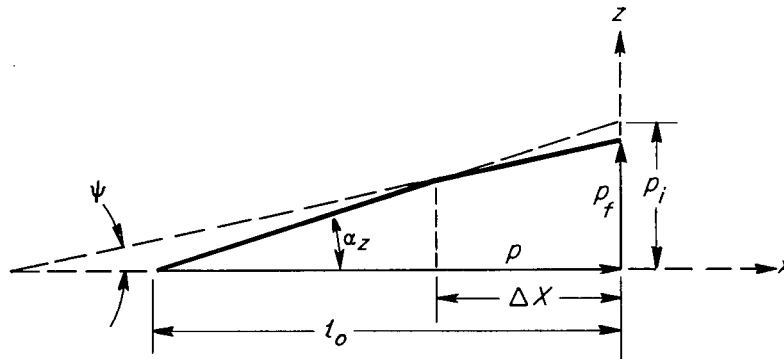


Fig. 6. Effect of Fringing Field on Vertical Focus Position.

8. THE SYMMETRIC ARRANGEMENT

If we require the ion trajectories to be symmetric about the plane $\phi = \Phi/2$ in addition to possessing mirror symmetry about the $z = 0$ plane, the equations expressing the image characteristics simplify. Under these conditions the object and image distances are equal, $\epsilon_1 = \epsilon_2 = \epsilon$,

⁴¹R. M. Sternheimer, *Rev. Sci. Instr.* 23, 629 (1952).

and $R_1 = R_2 = R$. The horizontal and vertical focusing equations, (77) and (83), now become

$$\frac{l_r}{r_0} = \frac{(1-n)^{1/2} \cot[(1-n)^{1/2} \Phi/2] + \tan \epsilon}{(1-n) - 2(1-n)^{1/2} \cot(1-n)^{1/2} \Phi \tan \epsilon - \tan^2 \epsilon} \quad (84)$$

and

$$\frac{l_z}{r_0} = \frac{n^{1/2} \cot(n^{1/2} \Phi/2) - \tan \epsilon}{n + 2n^{1/2} \cot n^{1/2} \Phi \tan \epsilon - \tan^2 \epsilon} \quad (85)$$

In the case of normal incidence, $\epsilon = 0$ and these focus conditions reduce to

$$l_r = r_0(1-n)^{-1/2} \cot[(1-n)^{1/2} \Phi/2] \quad (86)$$

and

$$l_z = r_0 n^{-1/2} \cot(n^{1/2} \Phi/2) \quad (87)$$

Equations (52), (53), and (78) for the magnification all reduce to unity, as they must, for the symmetric arrangement. Thus

$$M_r = M_z = 1 \quad (88)$$

The mass dispersion (79) reduces to

$$D_m = \frac{r_0}{1-n} \left\{ \frac{1 + (1-n)^{-1/2} \tan[(1-n)^{1/2} \Phi/2] \tan \epsilon}{1 - 2(1-n)^{-1/2} \cot(1-n)^{1/2} \Phi \tan \epsilon - (1-n)^{-1} \tan^2 \epsilon} \right\} \quad (89)$$

and for $\epsilon = 0$ becomes simply

$$D_m = \frac{r_0}{1-n} \quad (90)$$

The pole edge radius R required to make the second-order angular aberration terms A_{11} [Eq. (66)] vanish for $l_o = l_r$ and $\epsilon_1 = \epsilon_2 = 0$ is

$$R = \frac{3(1-n)^2 l_r^3}{3(1-n) r_0^2 - 2(n-b) [2r_0^2 + 3(1-n) l_r^2]} \quad (91)$$

For straight boundaries, $R = \infty$, and the field shape parameter b required to make $A_{11} = 0$ is given by

$$b = \frac{n[13 - \cos(1-n)^{1/2} \Phi] - 3[1 - \cos(1-n)^{1/2} \Phi]}{2[5 + \cos(1-n)^{1/2} \Phi]} \quad (92)$$

The total path length l from source to detector is $l = l_o + r_0 \Phi + l_r$. With $\epsilon_1 = \epsilon_2 = 0$, we may find the value of l_o which will minimize this path length for fixed values of n and Φ . Setting $\partial l / \partial l_o = 0$ and using Eq. (47) for l_r , one finds that the minimum path length (and hence maximum

transmission) is achieved for the symmetric case, $l_r = l_o$. For this case, as can be seen from (86), the total ion path length increases with increasing values of n but decreases as Φ becomes larger.

On the other hand, one may decrease the total ion path length for given values of n and Φ by choosing negative values of ϵ [see Eq. (84)]. However, the mass dispersion (89) also becomes smaller as ϵ becomes more negative. These ideas are illustrated in the numerical example shown in Table 1. If one considers transmission and dispersion simultaneously, one must conclude that the optimum symmetric arrangement is that for which $\epsilon = 0$. For this case one may use (91) together with (67) or (69) to achieve second-order radial focusing.

Table 1. Image Position and Mass Dispersion as a Function of n and ϵ for $\Phi = \pi$ and $l_r = l_o$

n	ϵ (deg)	l_r/r_0	D_m/r_0
0.8	0	2.71	5
0.9	0	5.84	10
	-5	3.86	6.62
	-10	2.87	4.93
	-15	2.27	3.91
	-20	1.86	3.24

9. SIMULTANEOUS DOUBLE DIRECTIONAL AND SECOND-ORDER RADIAL FOCUSING

To obtain double directional focusing the image distances l_r and l_z must be equal. By equating (77) and (83) Karmohapatra⁴² has worked out numerical values for l_o , ϵ_1 , and ϵ_2 which will produce horizontal and vertical focusing simultaneously for $\Phi = 180^\circ$ and for $n = 0.8$ and 0.9 . For example, first-order double directional focusing is achieved for $\Phi = 180^\circ$, $n = 0.8$, $\epsilon_1 = 60^\circ$, $\epsilon_2 = -19^\circ$, $l_o = 2r_0$, and $l_r = l_z = 3.5r_0$. Evaluating the mass dispersion for this case from (79) we find $D_m = 3.44r_0$. Using these same values for Φ and n in the symmetric case for $\epsilon = 0$, we find $D_m = 5.00r_0$ with essentially the same total path length from source to collector. This numerical example serves to illustrate the fact that double directional focusing is possible for any value of n within the allowable limits $0 \leq n < 1$ for the inflection-type asymmetric spectrometer. However, the accompanying reduction in the dispersion does not justify the experimentally awkward arrangement of source and collector which such a spectrometer would require.

For the case $\epsilon_1 = \epsilon_2 = 0$ it is apparent from (47) and (48) that simultaneous focusing is achieved for any combination of l_o and Φ provided $n = \frac{1}{2}$. Other values of n will also satisfy

⁴²S. B. Karmohapatra, *Indian J. Phys.* 29, 393 (1955); 32, 26 (1958).

the double focusing condition $l_r = l_z$ for at most one value of $\Phi < 2\pi$ for each $l_o \geq 0$. However, such a system lacks flexibility, and focusing characteristics in the vertical and radial directions would be widely different.

We conclude that double directional focusing is practical only in the symmetric case for $n = \frac{1}{2}$ and $\epsilon = 0$. Then from (86) and (87)

$$l_r = l_z = l_o = 2^{1/2} r_0 \cot 2^{-3/2} \Phi \quad (93)$$

Note that the source and collector are located on the edge of the field ($l_o = 0$) for $\Phi = 2^{1/2}\pi$, resulting in maximum transmission. This corresponds to the double focusing beta spectrometer proposed by Siegbahn and Svartholm.⁴³

With $n = \frac{1}{2}$, Eq. (91) gives the radius of the field boundary required for second-order focusing where b is chosen so as to eliminate the A_{44} or the A_{55} aberration terms. It follows from (67) that for the symmetric arrangement with $n = \frac{1}{2}$ the angular aberration term A_{44} vanishes if

$$b = \frac{3}{4(3 - \sin^2 2^{-3/2} \Phi)} \quad (94)$$

whereas the A_{55} term is zero for

$$b = \frac{1}{2 + \frac{2}{3} \cos 2^{-1/2} \Phi (2 - 3 \cos 2^{-1/2} \Phi)} \quad (95)$$

For rectilinear field boundaries b should be chosen to eliminate the radial angular aberration term A_{11} , in which case, from (92),

$$b = \frac{7 + 5 \cos 2^{-1/2} \Phi}{4(5 + \cos 2^{-1/2} \Phi)} \quad (96)$$

Note that for rectilinear field boundaries one cannot simultaneously eliminate the α_r^2 and α_z^2 aberration terms with a single value of the field parameter b . This same conclusion was reached by Shull and Dennison⁴⁴ for the special case $\Phi = 2^{1/2}\pi$.

10. FRINGE FIELD EFFECTS

Up to this point we have assumed rectilinear trajectories in the object and image regions, thereby neglecting the influence of the fringing field on the optical properties of inhomogeneous magnetic sector fields. The analysis of edge effects for homogeneous fields has been worked

⁴³K. Siegbahn and N. Svartholm, *Nature* 157, 872 (1946).

⁴⁴F. B. Shull and D. M. Dennison, *Phys. Rev.* 71, 681 (1947); 72, 256 (1947).

out by several authors.⁴⁵⁻⁵¹ Herzog^{52,53} suggests using suitable shields as a means of compensating for the influence of fringing fields. By analogy, these methods should be applicable to the case of inhomogeneous magnetic sector fields. However, we shall use the "factorization approximation" suggested by Judd and Bludman,⁵⁴ since this method is more directly applicable to the case of nonuniform fields.

The effects of fringing are:

1. The optic axes outside the magnet are bent through small angles, bringing the object and image closer together.
2. The object and image points are moved along the optic axis in the direction of the magnet.
3. The optimum values of the field shape parameters b, c, \dots which minimize second-order aberrations are modified from their values in the absence of fringing.

Mileikowsky⁵⁵ has experimentally determined the magnitude of effects 1 and 2 for the case of his nuclear spectrometer. To treat these effects quantitatively we must have a suitable approximate formula for the ion trajectories in the fringing regions.

Consider the motion of ions in the median plane ($z = 0$) where the magnetic induction is directed along the positive z axis. The equations of motion for particles in this x, y plane are then

$$m\ddot{x} = q\dot{y}B_z ,$$

$$m\ddot{y} = -q\dot{x}B_z ,$$

$$\dot{x}^2 + \dot{y}^2 = v^2 = \text{const} ,$$

where the dots denote differentiation with respect to time. Integrating the second equation once with respect to time we have

$$\dot{y} = -\frac{q}{m} \int B_z dx = -v \int \frac{B_z}{B_0} dx \equiv -v f(x, y) ,$$

⁴⁵N. D. Coggeshall, *J. Appl. Phys.* **18**, 855 (1947).

⁴⁶K. T. Bainbridge, *Phys. Rev.* **75**, 216 (1949).

⁴⁷K. T. Bainbridge, part V in *Experimental Nuclear Physics* (ed. by E. Segre), vol 1, Wiley, New York, 1953.

⁴⁸W. Ploch and W. Walcher, *Z. Physik* **127**, 274 (1950).

⁴⁹C. Reuterswärd, *Arkiv Fysik* **3**, 53 (1952).

⁵⁰L. A. König and H. Hintenberger, *Z. Naturforsch.* **10a**, 877 (1955).

⁵¹L. Kerwin, *Can. J. Phys.* **36**, 711 (1958).

⁵²R. Herzog, *Z. Physik* **97**, 596 (1935).

⁵³R. F. K. Herzog, *Z. Naturforsch.* **10a**, 887 (1955).

⁵⁴D. L. Judd and S. A. Bludman, *Nuclear Instr.* **1**, 46 (1957).

⁵⁵C. Mileikowsky, *Arkiv Fysik* **7**, 33 (1954).

where B_0 is the field within the gap at the equilibrium radius r_0 , and x and y are measured in units of r_0 . Now from the velocity equation we see that

$$\dot{x} = \pm v \left[1 - \left(\frac{\dot{y}}{v} \right)^2 \right]^{1/2} = \pm v(1 - f^2)^{1/2} .$$

Dividing these last two results we get the rigorous trajectory equation for ions in the $z = 0$ plane, namely,

$$\frac{\dot{y}}{\dot{x}} = \frac{dy}{dx} \equiv y' = \pm \frac{f}{(1 - f^2)^{1/2}} ,$$

or

$$\frac{d}{dx} \left[\frac{y'}{(1 + y'^2)^{1/2}} \right] = \pm \frac{B_z(x, y)}{B_0} . \quad (97)$$

As we have seen earlier, the symmetric arrangement of source and collector provides the most practical setup. We shall therefore confine our attention to such a system. The trajectories from a point source (for $\beta = 0$) are then completely symmetrical about the $\Phi/2$ plane, from which we shall now measure angles in terms of the coordinate θ . Referring explicitly to the image side, we choose the origin of the Cartesian coordinate system at

$$r = r_0 \quad \text{and} \quad \theta = \frac{\Phi}{2} - \phi .$$

The y axis is directed radially outward, with the particles moving in the direction of positive x ; ϕ is the small angle between the y axis and the magnet edge where fringing effects just begin and is of the order of g_0/r_0 , where g_0 is the gap width at r_0 . These ideas are illustrated in Fig. 7.

UNCLASSIFIED
ORNL-LR-DWG 45146

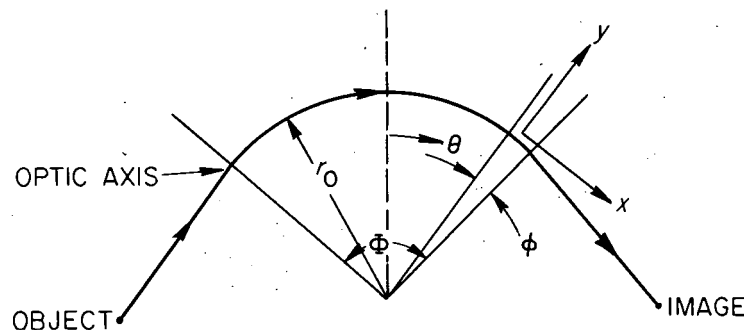


Fig. 7. Trajectory with Fringing Field.

Within the sector field the trajectories on the median plane for $\beta = 0$ may be found from Eq. (37). Remembering that the solution must be symmetric about the $\theta = 0$ plane we have

$$\rho = \rho_m D_1 + \rho_m^2 D_{11} = \rho_m \cos \theta_r + \frac{1}{6} \rho_m^2 [(X - 3) \sin^2 \theta_r + X(1 - \cos \theta_r)] , \quad (98)$$

where $X = 2(n - b)/(1 - n)$, $\theta_r = (1 - n)^{1/2} \theta$, and ρ_m is the displacement at $\theta = 0$. In the fringe field region the trajectories are given by (97), where the minus sign applies to the image space. We must match these trajectories along the y axis, which separates the domains of applicability. Now in both systems lengths are measured in units of r_0 , and so we have at $x = 0$

$$y = \rho , \quad y' = \frac{1}{r} \frac{dr}{d\theta} = \frac{\rho'}{1 + \rho} , \quad (99)$$

where ρ and ρ' are to be evaluated at $\theta = (\Phi/2) - \phi$.

Since the field on the median plane within the sector region varies as

$$B_z = B_0(1 - n\rho + b\rho^2 - \dots) ,$$

we assume that in the fringing region we may write

$$B_z(x, y) = (1 - ny + by^2 - \dots) \frac{g}{g_0} B_z(x) . \quad (100)$$

The g/g_0 term in the radial shape factor $(1 - ny + by^2 - \dots) g/g_0$ is needed to describe how the fringe field varies as a function of the gap width. This second factor is omitted by Judd and Bludman⁵⁴ in their treatment of the fringing field and accounts for the unrealistically large value they get for the image distance. Since

$$g_0 = \frac{2r_0}{n} \tan \frac{\gamma}{2} ,$$

as can be seen from Eq. (16),

$$\frac{g}{g_0} = \frac{r}{r_0} = 1 + y ,$$

making the radial shape factor

$$(1 - ny + by^2) \frac{g}{g_0} \approx 1 + (1 - n) y - (n - b) y^2 .$$

The shape factor is of the order of unity, and so we may use the rectilinear approximation

$$y = \rho + \frac{\rho'}{1 + \rho} x ,$$

where again ρ and ρ' are to be evaluated at $x = 0$. Now both ρ and ρ' are small compared with

unity, and so we write $y \approx \rho + \rho' x$ and $y^2 \approx \rho^2$. The shape factor now becomes

$$(1 - ny + by^2) \frac{g}{g_0} \approx 1 + (1 - n) \rho - (n - b) \rho^2 + (1 - n) \rho' x . \quad (101)$$

This factorization approximation [Eq. (100)] contains the assumption that the variation in the orientation of the axes within the small angle ϕ leads to effects of higher than second order.

Substituting (101) and (100) into (97) and integrating once, we obtain

$$\frac{y'}{(1 + y'^2)^{1/2}} = \frac{\rho'}{[(1 + \rho)^2 + \rho'^2]^{1/2}} - [1 + (1 - n) \rho - (n - b) \rho^2] f(x) - (1 - n) \rho' g(x) ,$$

where

$$f(x) \equiv \int_0^x \frac{B_z(x)}{B_0} dx \quad \text{and} \quad g(x) \equiv \int_0^x \frac{x B_z(x)}{B_0} dx .$$

Solving for y' and keeping terms through second-order approximation in ρ , this equation reduces to

$$y' = \rho'(1 - \rho) - \left[1 + (1 - n) \rho - (n - b) \rho^2 + \frac{3}{2} \rho'^2 \right] f - (1 - n) \rho' g + \frac{3}{2} \rho' [1 + (1 - 2n) \rho] f^2 - \frac{1}{2} f^3 + \dots . \quad (102)$$

Integrating once more we have

$$y = \rho + \rho'(1 - \rho) x - \left[1 + (1 - n) \rho - (n - b) \rho^2 + \frac{3}{2} \rho'^2 \right] \int_0^x f(x) dx - (1 - n) \rho' \int_0^x g(x) dx + \frac{3}{2} \rho' [1 + (1 - 2n) \rho] \int_0^x f^2(x) dx - \frac{1}{2} \int_0^x f^3(x) dx + \dots . \quad (103)$$

Since $B_z(x)$ is negligible near the image position x_0 , we may approximate $f(x)$, for x several times larger than g_0/r_0 , as follows:

$$f(x) \equiv \int_0^x \frac{B_z}{B_0} dx = c_1 a = \text{const} .$$

Choosing a as the distance over which the field falls off by one order of magnitude, c_1 is a

constant of the order of unity. Then

$$\left. \begin{aligned} \int_0^x f(x) dx &= c_1 ax + c_2 a^2 , \\ \int_0^x g(x) dx &= c_3 a^2 + c_4 a^3 , \\ \int_0^x f^2 dx &= c_1^2 a^2 x + c_5 a^3 . \end{aligned} \right\} \quad (104)$$

The additive constant terms $c_2 a^2$, $c_4 a^3$, and $c_5 a^3$ are correction factors arising from the fact that for small x ($x \leq a$)

$$\int_0^x \frac{B_x}{B_0} dx < c_1 a .$$

Integrating the second equation by parts shows that $c_2 = -c_3$. Now experimental measurements of the fringing fields indicate that a is of the order of a few gap widths. Therefore we may neglect terms in (103) which are of higher order than a^2 , since the c 's in (104) are near unity. The trajectories in the image space then become

$$\begin{aligned} y = \rho + \left[1 + (1-n)\rho - (n-b)\rho^2 + \frac{3}{2}\rho'^2 \right] c_3 a^2 + \\ + x \left\{ \rho'(1-\rho) - \left[1 + (1-n)\rho - (n-b)\rho^2 + \frac{3}{2}\rho'^2 \right] c_1 a + \right. \\ \left. + \frac{3}{2}\rho' [1 + (1-2n)\rho] c_1^2 a^2 - (1-n)\rho' c_3 a^2 \right\} . \end{aligned} \quad (105)$$

The constants $c_1 a$ and $c_3 a^2$ are determined by a numerical integration of the measured fringing field.

Ions moving on the equilibrium orbit determine the optic axis of the system. Thus the optic axis in the fringe field is given by (105) with $\rho = \rho' = 0$, that is,

$$y_{OA} = -c_1 ax + c_3 a^2 . \quad (106)$$

This equation displays the additional bending of the optic axis due to the fringing field.

The image position x_0 is located at that point where the paraxial ray crosses the optic axis. Thus we have

$$\begin{aligned} y(x_0) - y_{OA}(x) = 0 = \rho + \left[(1-n)\rho - (n-b)\rho^2 + \frac{3}{2}\rho'^2 \right] c_3 a^2 + x_0 \left\{ \rho'(1-\rho) - \right. \\ \left. - \left[(1-n)\rho - (n-b)\rho^2 + \frac{3}{2}\rho'^2 \right] c_1 a + \frac{3}{2}\rho' [1 + (1-2n)\rho] c_1^2 a^2 - (1-n)\rho' c_3 a^2 \right\} . \end{aligned}$$

Using (98) for ρ and classifying terms according to powers of ρ_m , neglecting third- and higher-order terms, we have

$$\begin{aligned} \rho_m \left(D_1 [1 + (1-n) c_3 a^2] + x_0 \left\{ D_1' \left[1 - (1-n) c_3 a^2 + \frac{3}{2} c_1^2 a^2 \right] - (1-n) D_1 c_1 a \right\} \right) + \\ + \rho_m^2 \left(D_{11} + \left[(1-n) D_{11} - (n-b) D_1^2 + \frac{3}{2} D_1'^2 \right] c_3 a^2 + \right. \\ \left. + x_0 \left\{ D_{11}' - D_1 D_1' - \left[(1-n) D_{11} - (n-b) D_1^2 + \frac{3}{2} D_1'^2 \right] c_1 a + \right. \right. \\ \left. \left. + \frac{3}{2} [D_{11}' + (1-2n) D_1 D_1'] c_1^2 a^2 - (1-n) D_{11}' c_3 a^2 \right\} \right) + \dots = 0 \quad (107) \end{aligned}$$

The D functions and their derivatives are to be evaluated along the y axis where $\theta = (\Phi/2) - \phi$.

For first-order focusing the coefficient of ρ_m must vanish. Hence

$$\begin{aligned} x_0 &= -\frac{D_1}{D_1'} \frac{1 + (1-n) c_3 a^2}{1 - (1-n) (D_1'/D_1) c_1 a + \frac{3}{2} c_1^2 a^2 - (1-n) c_3 a^2} \\ &= d \left\{ 1 - (1-n) d c_1 a - \left[\frac{3}{2} - (1-n)^2 d^2 \right] c_1^2 a^2 + 2(1-n) c_3 a^2 + \dots \right\}, \quad (108) \end{aligned}$$

where

$$d \equiv -\frac{D_1}{D_1'} = (1-n)^{-1/2} \cot \psi \quad \text{and} \quad \psi \equiv (1-n)^{1/2} \left(\frac{\Phi}{2} - \phi \right). \quad (109)$$

A simpler, though less rigorous, derivation of this result is presented in Appendix B.

Second-order radial focusing in the median plane may be achieved by selecting the field parameter b so that the term proportional to ρ_m^2 in (107) vanishes. Using (108) to eliminate x_0 in (107) and arranging terms according to powers of a , the condition for second-order radial focusing becomes

$$\begin{aligned} D_{11} + d(D_{11}' - D_1 D_1') - \left[(1-n) (D_{11}' - D_1 D_1') d + (1-n) D_{11} - (n-b) D_1^2 + \frac{3}{2} D_1'^2 \right] c_1 a d + \\ + \left\{ 3(1-n) D_1 D_1' - (1-n)^2 d^2 D_1 D_1' + (1-n)^2 d(D_{11} + dD_{11}') + \right. \\ \left. + (1-n) d \left[\frac{3}{2} D_1'^2 - (n-b) D_1^2 \right] \right\} c_1^2 a^2 d - \left[-(1-n) (D_{11} + dD_{11}') + \right. \\ \left. + 2(1-n) D_1 D_1' d + (n-b) D_1^2 - \frac{3}{2} D_1'^2 \right] c_3 a^2 + \dots = 0 \end{aligned}$$

Now in zero-order approximation the sum of terms independent of a must be zero, and so $D_{11} + d(D'_{11} - D_1 D'_1) \approx 0$. We may use this approximation to eliminate the D_{11} and D'_{11} terms in the coefficients of a and a^2 . With this approximation the above equation reduces to

$$D_{11} + d(D'_{11} - D_1 D'_1) - D_1^2 \left[\frac{3}{2}(1-n) \tan^2 \psi - (n-b) \right] c_1 a d + \\ + D_1^2 \left[(1-n) - (n-b) + \frac{3}{2}(1-n) \tan^2 \psi \right] c_3 a^2 - \\ - (1-n) D_1^2 \left[(n-b) + \frac{3}{2}(1-n) \tan^2 \psi \right] c_1^2 a^2 d^2 = 0 .$$

This equation determines the field parameter b required to produce second-order radial focusing in the median plane. The result may be written in the form

$$b = b_0 + b_1 + b_2 , \quad (110)$$

where

$$b_0 = \frac{13n - 3(1 - \cos 2\psi) - n \cos 2\psi}{2(5 + \cos 2\psi)} , \\ b_1 = - \frac{3(1-n)^2 (1 + \cos 2\psi)}{2(5 + \cos 2\psi)} \left[3 \tan^2 \psi - \frac{2(n-b_0)}{1-n} \right] c_1 a d , \\ b_2 = - \frac{3(1-n)^2 (1 + \cos 2\psi)}{2(5 + \cos 2\psi)} \left\{ (1-n) \left[3 \tan^2 \psi + \frac{2(n-b_0)}{1-n} \right] c_1^2 a^2 d^2 - \right. \\ \left. - \left[3 \tan^2 \psi - \frac{2(n-b_0)}{1-n} + 2 \right] c_3 a^2 \right\} ,$$

where again

$$\psi = (1-n)^{1/2} \left(\frac{\Phi}{2} - \phi \right) \quad \text{and} \quad d = (1-n)^{-1/2} \cot \psi .$$

The constants ϕ , $c_1 a$, and $c_3 a^2$ should be determined from a measurement of the fringing field. Experiments indicate that

$$\phi \approx \frac{2}{3} \frac{g_0}{r_0} , \quad c_1 a \approx \frac{5}{3} \frac{g_0}{r_0} , \quad c_3 a^2 \approx 3 \left(\frac{g_0}{r_0} \right)^2 .$$

Note that in the absence of fringing, $\phi = a = 0$ and Eqs. (108) and (110) reduce to

$$x_0 = (1-n)^{-1/2} \cot (1-n)^{1/2} \frac{\Phi}{2} , \\ b = \frac{n[13 - \cos (1-n)^{1/2} \Phi] - 3[1 - \cos (1-n)^{1/2} \Phi]}{2[5 + \cos (1-n)^{1/2} \Phi]} ,$$

which agree with our previous results (86) and (92), respectively. Having determined the optimum value of b necessary to eliminate the second-order radial aberration in the $z = 0$ plane, Eq. (14) gives the profile of the pole shoes required to produce this desired field shape.

11. A NUMERICAL ILLUSTRATION

We shall now use the foregoing results to estimate, theoretically, the focusing characteristics of the inhomogeneous field spectrometer currently under construction at this Laboratory. The magnet is designed for an equilibrium radius $r_0 = 12.0$ in. at a gap width $g_0 = 0.760$ in. To obtain $n = \frac{1}{2}$ for double directional focusing, conical pole shoes are used with the taper angle $\gamma/2 = 0.906^\circ$ as determined from Eq. (16). With the pole shoes cut for a sector angle of 90° , measurements indicated that the magnetic field begins to fringe at $\frac{1}{2}$ in. within the gap, and so

$$\phi = \frac{0.50}{12.0} = 0.0417 \text{ radian .}$$

A numerical integration of the B_z component of the measured fringing field in the $z = 0$ plane gives the results

$$c_1 a \equiv \int_0^{x_0} \frac{B_z}{B_0} dx = 0.104 ,$$

and

$$c_3 a^2 \equiv \int_0^{x_0} x \frac{B_z}{B_0} dx = 0.0122 .$$

Now, taking these values into consideration, a new sector angle was chosen so as to give a total deflection of the ion beam from source to collector equal to 90° . The pole edges were therefore trimmed to give a sector angle (see Fig. 8)

$$\Phi = \frac{\pi}{2} - 2(c_1 a - \phi) = 82.8^\circ .$$

With the source and the collector set at equal distances from the magnet edge, the coordinates of the image position (in units of r_0) are calculated from Eqs. (106) and (108). The results are

$$x_0 = 2.36 \quad \text{and} \quad y(x_0) = -0.234 .$$

We now estimate the magnitude of the second-order aberration terms. As was seen in Sec 2, $b = n^2$ for an ideal conical field. Neglecting fringing, we obtain from Eqs. (66) to (69)

$$A_{11} = 5.68r_0 ,$$

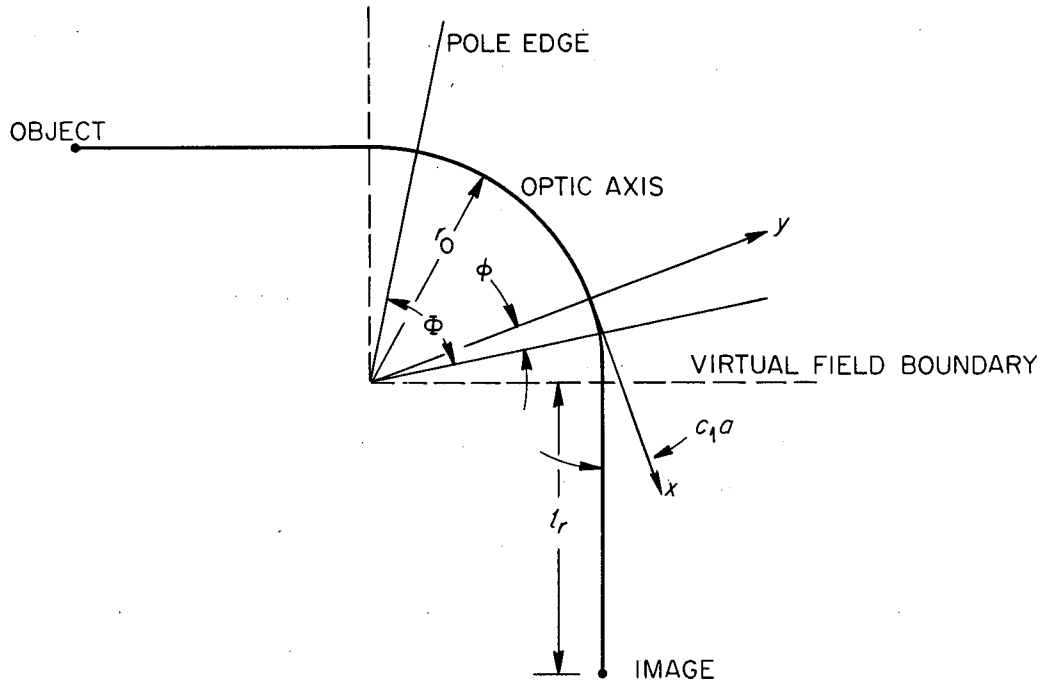


Fig. 8. Sector Field for 90° Deflection.

$$A_{44} = -0.66r_0 ,$$

$$A_{45} = -0.99 ,$$

$$A_{55} = \frac{-0.28}{r_0} .$$

Neglecting third- and higher-order aberrations as well as pressure broadening effects, the total beam width at the collector is

$$\text{B. W.} = M_r s_1 + \frac{r_0}{1-n} (1 + M_r) \frac{\delta V}{V} + \alpha_r^2 A_{11} + \alpha_z^2 A_{44} + \alpha_z \delta z A_{45} + (\delta z)^2 A_{55} ,$$

where s_1 is the source slit width and $M_r = 1$ for the symmetric arrangement of source and receiver. Using the parameters

$$\begin{aligned} s_1 &= 8 \times 10^{-3} \text{ in.} , & \frac{\delta V}{V} &= \frac{0.2}{5 \times 10^3} = 0.04 \times 10^{-3} , \\ r_0 &= 12.0 \text{ in.} , & \alpha_r &= 0.013 \text{ radian} , \\ \delta z &= 0.22 \text{ in.} , & \alpha_z &= 0.008 \text{ radian} , \end{aligned}$$

which are estimated from the source and tube dimensions, the estimated beam width is

$$\text{B. W.} = r_0 \times 10^{-3} (0.67 + 0.16 + 0.96 - 0.04 + 0.15 - 0.09) = 0.022 \text{ in.}$$

This beam width estimate is probably too large because of electrostatic focusing in the ion source, which tends to make the effective values of s_1 and a_r less than those calculated from the physical dimensions of the source. With a collector slit $s_2 = 16 \times 10^{-3}$ in., the calculated resolution (70) becomes

$$R = \frac{2r_0}{s_2 + \text{B.W.}} \approx 630 .$$

Note that in the absence of aberrations the resolution for these slit widths would be 1000. The linear dispersion between masses 235 and 236 may be calculated from (55). The result is

$$D = 2r_0 \frac{\delta m}{m} \approx 0.10 \text{ in.}$$

The value of b required to eliminate the A_{11} aberration term, which is the largest of the second-order aberrations, may be calculated from Eq. (110) with the result

$$b = b_0 + b_1 + b_2 = 0.4423 - 0.0175 - 0.0011 = 0.424 .$$

This calculation takes fringing effects into consideration and dictates the pole shoe profile, to be calculated from Eq. (14), needed to minimize second-order aberrations (see Table 2). With this modification the resolution would be increased to 910. One could also achieve second-order focusing with conical pole shoes by carefully choosing the sector angle Φ . For this case $b = n^2$, and so for $n = \frac{1}{2}$,

$$X = \frac{2(n - b)}{1 - n} = 1 .$$

Then the angle at which the second-order aberration term A_{11} disappears, neglecting fringing, may be found from (92), with the result

$$\Phi = 2^{3/2} \frac{\pi}{3} = 169.3^\circ .$$

One could also make the A_{11} aberration coefficient vanish by proper shaping of the pole boundary. For this symmetric system the required radius, as calculated from Eq. (91), is -14.6 in. The negative sign implies that the pole boundaries are concave with respect to the object and image points. This result is of questionable significance, since here the effects of fringing have been neglected.

Mileikowsky⁵⁶ has suggested an empirical procedure for locating the image position in the fringing field. One imagines that the system behaves as an ideal magnetic lens (no fringing) with an "effective" sector angle equal to the angle between the initial and final directions of the ion beam so that r_0 in the sector field is the same with and without fringing. He has found that the image position calculated in this manner agrees well with experimental observations. In our

⁵⁶C. Mileikowsky, *Arkiv Fysik* 7, 33 (1954).

Table 2. Shape of Pole Shoes

$$n = \frac{1}{2}$$

$$g_0 = 0.760 \text{ in.}$$

$$r_0 = 12.00 \text{ in.}$$

z coordinate measured from median plane

r (in.)	z (in.)		r (in.)	z (in.)	
	For $A_{11} = 0^*$	For Conical Pole Faces		For $A_{11} = 0^*$	For Conical Pole Faces
9.000	0.3301	0.3325	12.200	0.3831	0.3832
9.250	0.3343	0.3364	12.400	0.3863	0.3863
9.500	0.3386	0.3404	12.500	0.3878	0.3879
9.750	0.3428	0.3444	12.750	0.3916	0.3919
10.000	0.3470	0.3483	13.000	0.3953	0.3958
10.250	0.3512	0.3523	13.250	0.3990	0.3998
10.500	0.3554	0.3562	13.500	0.4025	0.4038
10.750	0.3596	0.3602	13.750	0.4060	0.4077
11.000	0.3638	0.3642	14.000	0.4093	0.4117
11.250	0.3679	0.3681	14.250	0.4126	0.4156
11.500	0.3720	0.3721	14.500	0.4157	0.4196
11.600	0.3736	0.3737	14.750	0.4187	0.4236
11.800	0.3768	0.3768	15.000	0.4216	0.4275
12.000	0.3800	0.3800			

*Requires $b = 0.4237$.

case the effective sector angle is 90° . As can be seen in Fig. 8, the virtual field boundary is displaced at an angle $c_1 a$ from the y axis. The image distance as measured from this virtual boundary may be calculated from (86), with the result

$$l_r = r_0 (1 - n)^{-1/2} \cot \left[(1 - n)^{1/2} \frac{\pi}{2} \right] = 27.4 \text{ in.}$$

From our previous calculations we obtain

$$l_r = r_0 (x_0 - c_1 a) = 27.1 \text{ in.}$$

Although the more rigorous mathematical treatment, based on the "factorization" approximation, gives a slightly smaller answer, the two methods yield essentially the same result. These findings are in qualitative agreement with Mileikowsky's observation⁵⁶ that the optimum focus position as determined experimentally is somewhat less than that predicted by the "effective" sector angle treatment.

With Φ taken as 90° , Eq. (92) gives $b = 0.425$ as the field shape parameter needed to eliminate the A_{11} aberration. This result is also in good agreement with our previous calculation, from which we found $b = 0.424$. If one completely neglects the fringing field, the required field shape parameter for second-order focusing is calculated to be $b = 0.442$. This result suggests that one cannot ignore the fringing field when correcting for second-order aberrations.

12. CONCLUSION

Theoretically, nonuniform magnetic fields which vary in first order as r^{-n} in the median plane may be used to increase the dispersion and resolving power in mass spectrometers by a factor of $(1 - n)^{-1}$ when compared with corresponding homogeneous field ($n = 0$) instruments. This potential improvement in resolution, however, is misleading unless steps are taken to reduce image aberrations. The chromatic aberration, proportional to $\delta V/V$, varies as $(1 - n)^{-1}$ and so is enhanced for the case of nonuniform magnetic lens systems. The most important second-order aberration term, that proportional to α_r^2 , is more than five times as large as the corresponding term in a homogeneous field spectrometer for the example given in the last section. For the same values of r_0 , s_1 , s_2 , and $\delta V/V$ used in this illustration, the estimated resolution for a conventional spectrometer is 440, which is only 30% less than that calculated for the $n = \frac{1}{2}$ field.

In principle, second-order radial focusing can be obtained by proper shaping of either the pole faces or the pole boundaries. Shaping of the pole faces appears to be the more desirable procedure, since one can then take into account the effect which the fringing field has on second-order focusing. With this modification, the resolution for the instrument described in the last section should be nearly twice that for the corresponding homogeneous field spectrometer. This example serves to illustrate the importance of the second-order geometric aberrations characteristic of inhomogeneous magnetic fields. Further improvement in the resolution is possible if the chromatic aberration term is reduced through the use of an electrostatic velocity filter or through the use of larger accelerating potentials.

The length of the central ion path is proportional to $(1 - n)^{-1/2}$. For a given n , the symmetric arrangement of source and collector gives the shortest ion path. Since the central path length is longer with the inhomogeneous field than with the homogeneous field, it appears that vacuum requirements are more rigid for the nonuniform magnetic field spectrometer if one is to obtain the same peak broadening due to residual gas in the analyzer tube.

For a given n , maximum dispersion is obtained for the case where the ion path enters and leaves the field boundaries at right angles. Double directional and second-order radial focusing may be achieved simultaneously by choosing $n = \frac{1}{2}$ and by properly shaping the pole faces.

The factorization approximation together with the improved radial shape factor appears to give a very satisfactory description of the effects produced by the magnetic fringing field. Not only does this method permit one to predict the modification in the focal position which the fringe field produces, but one can also calculate the field shape parameter required for second-order radial focusing taking edge effects into consideration. To a good approximation, one may

empirically account for these fringing effects in terms of an "effective" sector angle taken as the angle between the initial and final directions of the ion path, provided the ion path radius in the sector field is the same with and without fringing.

Appendix A

SUMMARY OF NOTATION

$\mathbf{A} \equiv$ magnetic vector potential.

$$\left. \begin{array}{l} \alpha_r^2 A_{11} \\ \alpha_z^2 A_{44} \\ \alpha_z \delta z A_{45} \\ (\delta z)^2 A_{55} \end{array} \right\} \equiv \text{second-order radial aberrations.}$$

$\mathbf{B} \equiv$ magnetic induction field.

$B_0 \equiv$ field on the median plane at r_0 .

$b \equiv$ coefficient of the quadratic term in the series expansion of the magnetic field.

$$c_1 a \equiv \int_0^{x_0} \frac{B_z}{B_0} dx.$$

$$c_3 a^2 \equiv \int_0^{x_0} x \frac{B_z}{B_0} dx.$$

$D \equiv$ lateral displacement of the ion beam in the y direction at the image position.

$D_E \equiv$ energy dispersion or chromatic aberration.

$$D_m \equiv \text{mass dispersion} \equiv \frac{D}{\delta m/m_0}.$$

$g_0 \equiv$ gap width at r_0 .

$l_o \equiv$ object distance measured from field boundary.

$l_r \equiv$ image distance for radial focusing.

$l_z \equiv$ image distance for vertical focusing.

$M_r \equiv$ radial magnification.

$M_z \equiv$ vertical magnification.

$m \equiv$ mass of the ion.

$n \equiv$ coefficient of the linear term in the series expansion of the magnetic field.

$p \equiv$ linear momentum of the ion.

$q \equiv$ charge of the ion.

$R \equiv$ mass resolving power.

$R_1 \equiv$ radius of curvature of the field boundary on the object side.

$R_2 \equiv$ radius of curvature of the field boundary on the image side.

$r \equiv$ radial coordinate in the cylindrical polar coordinate system used to describe the motion of the ion within the magnetic field.

r_0 \equiv radius of the central or equilibrium path.

s_1 \equiv source slit width.

s_2 \equiv receiver slit width.

V \equiv potential difference through which the ion has been accelerated.

X \equiv Tasman's field shape parameter $\equiv \frac{2(n-b)}{1-n}$.

x_0 \equiv radial image position in units of r_0 as measured from the axis within the gap at which fringing begins.

δy \equiv horizontal source dimension.

z \equiv axial coordinate in the cylindrical polar coordinate system used to describe the motion of the ion within the magnetic field. On the midplane within the pole gap $z = 0$, and the positive z axis is taken along the direction of the field.

δz \equiv vertical source dimension.

α_r \equiv semidivergent angle of the paraxial rays from the source as measured in the radial plane.

α_z \equiv semidivergent angle of the paraxial rays from the source as measured in the axial plane.

β \equiv momentum spread factor.

γ \equiv angle between the extensions of the conical pole pieces.

ϵ_1 \equiv angle made by the central ion path with the normal to the pole edge on the entrance side of the magnet.

ϵ_2 \equiv angle made by the central ion path with the normal to the pole edge on the exit side of the magnet.

$$\eta \equiv \left(\frac{q}{2mV} \right)^{1/2}$$

θ \equiv angle coordinate as measured from the $\Phi/2$ plane for the symmetric arrangement of source and collector.

ρ \equiv dimensionless radial coordinate $\equiv (r - r_0)/r_0$.

ρ' $\equiv d\rho/d\phi$.

ρ_0 \equiv value of ρ at $\phi = 0$.

ρ'_0 \equiv value of ρ' at $\phi = 0$.

ρ_m \equiv maximum value of ρ for the symmetric arrangement.

σ \equiv dimensionless axial coordinate $\equiv z/r_0$.

σ' $\equiv d\sigma/d\phi$.

σ_0 \equiv value of σ at $\phi = 0$.

σ'_0 \equiv value of σ' at $\phi = 0$.

Φ \equiv magnetic field sector angle.

ϕ \equiv polar angle in the cylindrical polar coordinate system used to describe the motion of the ion within the magnetic field.

ϕ_m \equiv magnetic scalar potential.

Appendix B

IMAGE DISPLACEMENT DUE TO FRINGING FIELD – A SIMPLIFIED ANALYSIS

A simplified, though less rigorous, estimate of the image displacement due to the fringing field is presented here. Using the same coordinate system as defined in Fig. 7, we see that in the midplane the y component of the magnetic force on the ion is given by

$$F_y = qv_x B_z(x, y) \approx -qv_x(1 - n\rho) B_z(x) .$$

Assuming the field falls from its maximum value to zero in a distance Δx , the relative change of momentum of an ion passing through this distance in time Δt is

$$\frac{\Delta p_y}{p} = \frac{F_y \Delta t}{p} \approx \frac{\Delta x F_y}{v_x p} \approx -(1 - n\rho) \frac{\Delta x}{r_0} .$$

Now Δx is of the same order of magnitude as the gap width, and so we write

$$\Delta x = Cg = Cg_0(1 + \rho) ,$$

where C is a constant of order unity. Hence

$$\frac{\Delta p_y}{p} \approx -(1 - n\rho)(1 + \rho) \frac{Cg_0}{r_0} \approx -[1 + (1 - n)\rho] \frac{Cg_0}{r_0} .$$

Now $\Delta p_y/p$ is just the change of slope of the ion trajectory produced by the fringing field. Setting $\rho = 0$ we get the slope of the optic axis, namely,

$$\left(\frac{\Delta p_y}{p} \right)_{\text{OA}} = - \frac{Cg_0}{r_0} .$$

Comparing this result with Eq. (106) we are able to make the identification

$$\frac{Cg_0}{r_0} = c_1 a .$$

Now the difference in slope change between the paraxial trajectory ($\rho \neq 0$) and the optic axis ($\rho = 0$) produced by the fringing field is just

$$\left(\frac{\Delta p_y}{p} \right)_{\rho} - \left(\frac{\Delta p_y}{p} \right)_{\text{OA}} = -\rho(1 - n) c_1 a .$$

Without fringing the image distance would be $d = -\rho/\rho'$, where $\rho = \rho_m \cos(1 - n)^{1/2} \theta$ and is to be evaluated along the y axis. Thus with fringing,

$$x_0 = - \frac{\rho}{\rho' - \rho(1 - n) c_1 a} = \frac{d}{1 + (1 - n) c_1 a d} = d[1 - (1 - n) c_1 a d + (1 - n)^2 c_1^2 a^2 d^2 - \dots] .$$

This result is essentially equivalent to Eq. (108) as obtained by the more rigorous treatment.

Appendix C

THE HOMOGENEOUS FIELD SPECTROMETER

The image characteristics for the inhomogeneous magnetic field spectrometer are perfectly general and reduce to the corresponding equations for the homogeneous case where $n = b = 0$. Thus the radial focus condition (77) for $n = 0$ becomes

$$r_0 \sin \Phi + \frac{l_0 \cos (\Phi - \epsilon_1)}{\cos \epsilon_1} + l_r \left\{ \frac{\cos (\Phi - \epsilon_2)}{\cos \epsilon_2} - \frac{l_0 \sin [\Phi - (\epsilon_1 + \epsilon_2)]}{r_0 \cos \epsilon_1 \cos \epsilon_2} \right\} = 0 ,$$

which is Herzog's well-known focus requirement.^{57,58} The vertical focusing resulting from the fringe field is given by (83) and with $n = 0$ becomes

$$\frac{l_z}{r_0} = \frac{\Phi + (l_0/r_0) (1 - \Phi \tan \epsilon_1)}{(l_0/r_0) [\tan \epsilon_1 + (1 - \Phi \tan \epsilon_1) \tan \epsilon_2] - (1 - \Phi \tan \epsilon_2)} ,$$

which is equivalent to the expressions derived by Cotte,⁵⁹ Camac,⁶⁰ and Cross.⁶¹

The aberration term A_{11} (66) reduces to Hintenberger's result^{62,63} for $n = b = 0$ and $\epsilon_1 = \epsilon_2 = 0$. If $R_1 = R_2 = \infty$, $A_{11} = -r_0$, which is valid for any symmetric homogeneous magnetic field spectrometer.

⁵⁷R. Herzog, *Z. Physik* **89**, 447 (1934).

⁵⁸J. Mattauch and R. Herzog, *Z. Physik* **89**, 786 (1934).

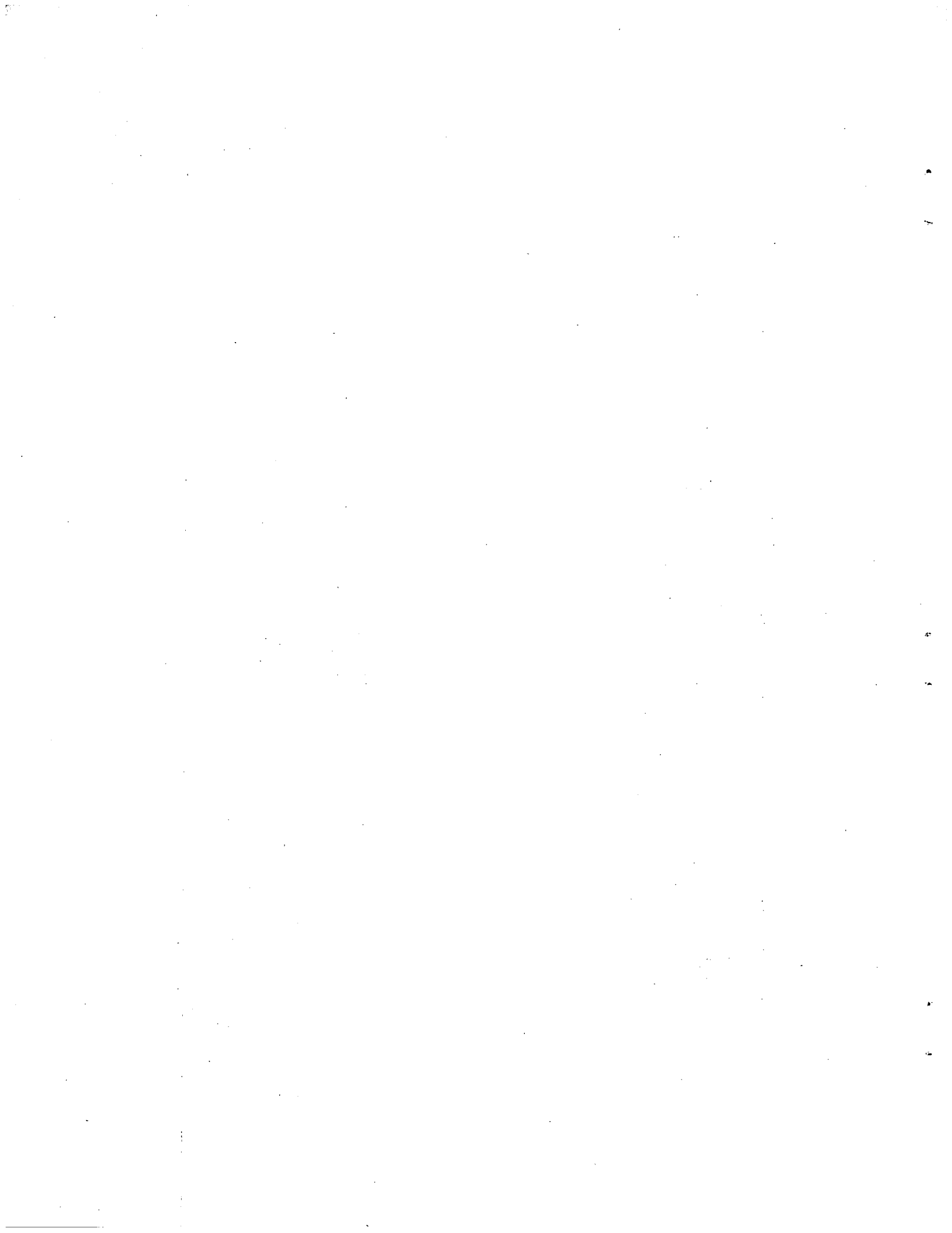
⁵⁹M. Cotte, *Ann. phys.* **10**, 333 (1938).

⁶⁰M. Camac, *Rev. Sci. Instr.* **22**, 197 (1951).

⁶¹W. G. Cross, *Rev. Sci. Instr.* **22**, 717 (1951).

⁶²H. Hintenberger, *Z. Naturforsch.* **3a**, 125, 669 (1948); **6a**, 275 (1951).

⁶³H. Hintenberger, *Rev. Sci. Instr.* **20**, 748 (1949).



INTERNAL DISTRIBUTION

1. C. E. Center
2. Biology Library
3. Health Physics Library
- 4-5. Central Research Library
6. Reactor Experimental
Engineering Library
- 7-26. Laboratory Records Department
27. Laboratory Records, ORNL R.C.
28. A. M. Weinberg
29. L. B. Emler (K-25)
30. J. P. Murray (Y-12)
31. J. A. Swartout
32. E. H. Taylor
33. E. D. Shipley
34. M. L. Nelson
35. M. T. Kelley
36. C. P. Keim
37. W. H. Jordan
38. F. L. Culler
39. S. C. Lind
40. A. H. Snell
41. A. Hollaender
42. K. Z. Morgan
43. T. A. Lincoln
44. A. S. Householder
45. R. S. Livingston
46. D. S. Billington
47. C. E. Winters
48. H. E. Seagren
49. D. Phillips
50. J. A. Lane
51. M. J. Skinner
52. J. M. Schreyer
53. G. E. Boyd
54. C. L. Burros
55. J. H. Cooper
56. L. T. Corbin
57. C. Feldman
58. D. J. Fisher
59. U. Koskela
60. W. R. Laing
61. C. E. Lamb
62. P. M. Reyling
63. R. S. Cockreham
64. G. C. Williams
65. D. E. LaValle
66. G. W. Leddicotte
67. S. A. Reynolds
68. P. F. Thomason
69. T. E. Willmarth
70. G. R. Wilson
71. E. I. Wyatt
72. L. J. Brady
73. H. P. House
74. J. R. Lund
75. E. C. Lynn
76. O. Menis
77. A. S. Meyer
78. C. D. Susano
79. C. K. Talbott
80. W. F. Vaughn
81. J. C. White
82. H. P. Raaen
83. J. A. Norris
84. D. L. Manning
85. T. C. Rains
- 86-100. A. E. Cameron
101. J. F. Burns
102. C. R. Baldock
103. G. Wells
104. C. Melton
105. J. Sites
106. E. J. Spitzer
107. J. R. Walton
108. W. H. Christie
109. E. F. Blase
110. J. S. Drury
111. F. C. Uffleman (Y-12)
112. W. D. Harmon (Y-12)
113. L. A. Smith (K-25)
114. H. A. Laitinen (consultant)
115. W. W. Meinke (consultant)
116. D. N. Hume (consultant)
117. C. E. Larson (consultant)
118. N. H. Furman (consultant)
119. L. L. Merritt (consultant)
120. ORNL - Y-12 Technical Library
Document Reference Section

EXTERNAL DISTRIBUTION

- 121. Division of Research and Development, AEC, ORO
- 122. Knolls Atomic Power Laboratory (T. L. Collins, Jr.)
- 123. Argonne National Laboratory (C. M. Stevens)
- 124. Hanford Atomic Products Operation (R. Lagergren)
- 125. U.S. Geological Survey, Denver (R. Cannon)
- 126. National Bureau of Standards, Washington (F. L. Mohler)
- 127. Dept. of Physics, Institute of Technology, University of Minnesota, Minneapolis,
(A. O. C. Nier)
- 128. Iowa State University, Ames (H. Svec)
- 129. Major Keith O. Hamby, Headquarters, USAF, McClellan Air Force Base, California
- 130. U.S. Geological Survey, National Bureau of Standards, Washington (L. R. Stieff)
- 131-145. Valparaiso University, Valparaiso, Indiana (M. M. Bretscher)
- 146. General Electric Company, Vallicitos (W. Duffy)
- 147-756. Given distribution as shown in TID-4500 (15th ed.) under Physics and Mathematics
(75 copies - OTS)